

Annual Review of Biophysics

Giant Vesicles and Their Use in Assays for Assessing Membrane Phase State, Curvature, Mechanics, and Electrical Properties

Rumiana Dimova

Max Planck Institute of Colloids and Interfaces, Science Park Golm, 14424 Potsdam, Germany;
email: rumiana.dimova@mpikg.mpg.de

Annu. Rev. Biophys. 2019. 48:93–119

First published as a Review in Advance on
February 27, 2019

The *Annual Review of Biophysics* is online at
biophys.annualreviews.org

<https://doi.org/10.1146/annurev-biophys-052118-115342>

Copyright © 2019 by Annual Reviews.
All rights reserved

ANNUAL
REVIEWS **CONNECT**

www.annualreviews.org

- Download figures
- Navigate cited references
- Keyword search
- Explore related articles
- Share via email or social media

Keywords

model membranes, membrane domains, microcompartments, membrane elasticity, spontaneous curvature, membrane pores, phase diagrams, membrane tubes, electroporation

Abstract

Giant unilamellar vesicles represent a promising and extremely useful model biomembrane system for systematic measurements of mechanical, thermodynamic, electrical, and rheological properties of lipid bilayers as a function of membrane composition, surrounding media, and temperature. The most important advantage of giant vesicles over other model membrane systems is that the membrane responses to external factors such as ions, (macro)molecules, hydrodynamic flows, or electromagnetic fields can be directly observed under the microscope. Here, we briefly review approaches for giant vesicle preparation and describe several assays used for deducing the membrane phase state and measuring a number of material properties, with further emphasis on membrane reshaping and curvature.

Contents

1. INTRODUCTION	94
2. THE MAKING OF	95
2.1. One Classification of the Preparation Methods	96
2.2. Vesicle Swelling	96
2.3. Methods Based on the Use of an Oil Phase	97
2.4. More Complex Membranes, Protein Reconstitution, and Biomolecule Encapsulation	98
3. PHASE STATE OF MULTICOMPONENT MEMBRANES	98
3.1. Phase Diagrams	99
3.2. Critical Points and Tie Lines	100
3.3. Factors Affecting the Phase Diagrams of Lipid Mixtures	100
4. SOME ASSAYS FOR VESICLE MANIPULATION AND ASSESSING THE MEMBRANE MECHANICAL AND ELECTRICAL PROPERTIES	100
4.1. Fluctuation Analysis	101
4.2. Micropipette Aspiration and Injection	101
4.3. Membrane Properties and Interactions Assessed from Exposing Giant Vesicles to Electric Fields	103
4.4. All-Optical Assays for Measuring the Bending Rigidity, Membrane Fluidity, and Viscosity	105
4.5. Pulling Membrane Tubes	105
5. MEMBRANE CURVATURE AND VESICLE SHAPE	106
5.1. Spontaneous Curvature of Membranes	107
5.2. Membrane Versus Monolayer Curvature	107
5.3. Membrane Remodeling by Proteins, Solutes, and Lipids	108
5.4. Measuring the Membrane Spontaneous Curvature	108
6. OUTLOOK	109

1. INTRODUCTION

Cells typically have sizes in the range of 1 to 10 μm , which makes them visible with optical microscopy. The boundary ensuring their autonomy (i.e., the plasma membrane, which regulates a number of processes essential for the cell survival) has a comparable projected size. If we were able to empty the cell interior while controllably modulating the composition of the resulting capsule of lipids, membrane proteins, and other species, we would be able to better understand the biophysics of these membranes as well as the specific pathways that they govern, as these capsules would then be directly visible under a microscope and amenable to manipulation. We cannot do that (yet), but we can use giant vesicles, either synthetic (i.e., prepared from a starting well-defined mixture of molecules) or derived from the plasma membrane of cells. The former method represents a bottom-up approach of building a mimetic cell membrane, which can then be used to characterize the membrane properties or resolve the action of certain molecule(s) and environmental factors. This approach produces a well-controlled system because all players are known, but it is drastically limited in terms of complexity. The latter method, deriving the plasma membrane from cells, represents a top-down approach that reduces the cell membrane complexity by stripping it off from the adjacent cytoskeleton and isolates it from a large number of processes in

which it is involved during the cell life. Data collected on such complex systems exhibit strong noise owing to the enormous number of membrane components, which could be reacting simultaneously to perturbations. On the contrary, synthetic giant vesicles can be prepared from certain mixtures and thus provide the freedom to select specific components, where the role of each is of interest to the researcher. This review focuses on such synthetic giant unilamellar vesicles (GUVs) (43, 45, 48, 59, 123, 202), their use in resolving the material properties on cell membranes, and some of their applications in addressing membrane responses and functions.

Vesicles represent one of the many model membrane systems employed for resolving the membrane structure and its characterization. Examples of other model membranes include lipid monolayers at the air–water interface, solid supported bilayers, black lipid membranes, and bilayer stacks. Compared to these, vesicles or liposomes are the most natural system, because, shape- and structure-wise, they are closest to membranes of cells and cell organelles. Contrary to other model membrane systems, such as supported lipid bilayers or black lipid membranes, vesicles allow for control over the membrane tension [for giant vesicles, this control can be directly exercised by micropipette aspiration; osmotic inflation or deflation can also be used, but with lesser precision (81)]. Furthermore, black lipid membranes usually retain traces of the organic solvent used for their formation. The use of supported bilayers as model membranes typically raises concerns about steric hindrance or effects arising from the support. None of these disadvantages apply to vesicles.

Vesicles are typically classified according to multilamellarity (i.e., unilamellar and multilamellar), as well as according to size: Small unilamellar vesicles (SUVs) are a few tens of nanometers in size, and large unilamellar vesicles (LUVs) are in the hundred nanometer range. Compared to SUVs and LUVs, the GUVs are 10–1,000 times larger. GUVs employed for microscopy studies have sizes typically in the range of 10 to 100 μm , which makes them a handy biomimetic tool for directly displaying the response of the membrane on a cell-size scale. They can be observed under an optical microscope using various enhancement techniques such as phase contrast, differential interference contrast, or confocal and standard fluorescence microscopy, the latter two being particularly useful in, for example, distinguishing domains on multicomponent membranes (**Figure 1**). Higher-resolution techniques are less often applied to imaging GUVs as these are prone to hydrodynamic perturbations and require some kind of immobilization to allow imaging with precision in the nanometer range.

Since the first studies reporting observations on giant vesicles in 1969 (152), GUVs have developed into a rich research field (48). Because of the increasing interest and number of publications on giant vesicles in recent years, it is unavoidable that some studies are unintentionally omitted here. In this review, we briefly review methods for giant vesicle preparation and phase-state characterization. Then, we introduce several different approaches and techniques for assessing the membrane material properties. That is followed by a more extensive discussion on membrane reshaping and curvature generation.

2. THE MAKING OF

The development of methods for GUV preparation represents a particularly active area of research (for reviews, see 48, 139, 186, 194, 202). Methods are adjusted and optimized depending on the requirements for the GUV use and system properties. In some applications, the membrane composition is crucial, and traces of substances used for the preparation (e.g., organic phase) are undesirable, as they can strongly influence the membrane mechanical properties and phase state. In other applications, it is the size and solution composition inside and outside that are more important (e.g., when one aims to ensure conditions that are more physiologically relevant, or to

establish encapsulation of biomolecules). Finally, practical aspects such as time, yield, required materials, and setups, as well as cost, are also relevant factors for choosing a suitable method. A couple of approaches have been developed to establish control on the vesicle monodispersity (e.g., 101, 190); however, whether the GUV size distribution is preserved after harvesting the vesicles from the formation chambers is questionable.

2.1. One Classification of the Preparation Methods

The available protocols used for preparing GUVs have been previously organized in a number of different methods (202). Here, we conceptually divide them into vesicle swelling methods and methods based on the use of an oil/organic phase, as discussed in detail below. This classification is based on the following. (a) One starts by depositing lipids in organic solvent (e.g., chloroform) onto a solid or gel substrate, the solvent is evaporated, and then lipid hydration and swelling occur through the addition of an aqueous solution to form GUVs. Or (b) one takes advantage of the fact that GUVs are micrometer-sized (bilayer-encapsulated) aqueous droplets in a bulk aqueous media; to obtain the GUVs, one manipulates and combines two lipid monolayers at oil–water interfaces to form a bilayer enclosing quasi water-in-water droplets (i.e., GUVs) while removing the oil phase (most of the time, not completely) (see Section 2.3). In the following sections, we discuss in more detail each of these approaches. An alternative approach that does not seem to enter either of the above classifications relies on the deposition of the lipid bilayer onto the fluid substrate of a surfactant monolayer at the inner interface of an aqueous droplet in fluorinated oil, thus forming droplet-supported GUVs (205). The bilayer deposition is established similarly to how solid supported bilayers are formed—by spreading LUVs onto the substrate in the presence of divalent ions, but here, the substrate is a fluid interface. A combination of microfluidic manipulation and electroinjection allows the encapsulation of biomacromolecules and the building of cytoskeletal mimetics as well as the reconstitution of transmembrane proteins (205). Most importantly, the vesicles can also be successfully harvested from the droplets.

In all approaches, one should be aware of potential artifacts stemming from the preparation method and, depending on the application of the produced GUVs, decide whether to neglect these artifacts. For example, certain preparation conditions can lead to phospholipid degradation and inclusion of impurities in the vesicles deriving from the substrate or from the phase on which they were prepared, or even from the aqueous medium (28, 35, 95, 112, 126, 156, 192).

2.2. Vesicle Swelling

In this section, we focus on swelling that either occurs spontaneously or is enhanced by external forces such as electric fields, heat, and osmotic flow. More unconventional and less applicable methods also exist. For example, GUVs have also been prepared from preformed LUVs via fusion but at very high salt concentrations and under the application of freeze–thawing cycles (135).

2.2.1. Spontaneous swelling. The simplest version of the vesicle swelling method is referred to as spontaneous swelling and was initially applied to egg yolk phosphatidylcholines or their mixtures with cholesterol (152). As summarized above, the dissolved lipids are deposited on the solid substrate (e.g., glass or Teflon surface), the organic solvent is evaporated, the swelling buffer is added, and vesicles are produced within approximately one day. For details and video material on one specific protocol, see Reference 98 (if a picture is worth a thousand words, a video is worth even more, especially as protocols are not described in sufficient detail in publications). Inclusion

of charged lipids was reported to improve the vesicle preparation in physiological conditions (3). The use of sugars already present in the deposited lipid film was also shown to be beneficial (193) as were a number of other factors such as the presence of divalent ions in the aqueous solution (4), localized heating (22), and pressure waves (141). Swelling of GUVs on glass beads as a support was also demonstrated to allow for encapsulation of a minimal gene expression system (134).

2.2.2. Electroswelling. The swelling of the vesicles can be enhanced and sped up (to ~ 1 – 2 h) through the application of an external alternating current (AC) electric field. This approach is also called vesicle electroformation (8), whereby the lipids are deposited on electrically conductive solid surfaces acting as electrodes. These can be semiconductive glass plates coated with indium tin oxide (ITO), platinum, titanium, or stainless steel wires as well as silicon substrates (e.g., as employed in 11, 101, 121, 124, 143, 148). For egg phosphatidylcholine, electroformation was also shown to be feasible with lipid deposition on nonconductive substrates immersed between electrodes (136). The method was also found applicable for the preparation of GUVs with reconstituted proteins (video material is available in 64, 164).

2.2.3. Gel-assisted swelling. Vesicle swelling in the absence of electric field is slow (~ 1 – 2 days) but can be dramatically sped up (~ 1 – 30 min) when one uses a polymer-based gel as a substrate. The vesicle growth in gel-assisted methods is enhanced by buffer influx from below the bilayers that are swelling on a porous polymer layer. The method was first demonstrated on agarose gels (85), but agarose molecules trapped inside during the vesicle formation were found to alter the physicochemical properties of the GUVs (112). An improved version of the gel-assisted method replaced agarose with polyvinyl alcohol (PVA), circumventing polymer encapsulation, as the lipids do not penetrate the PVA film (204). More recently, chemically cross-linked dextran–poly(ethylene glycol) was used as hydrogel substrate for GUV preparation under physiological ionic strength conditions (125).

2.3. Methods Based on the Use of an Oil Phase

These methods rely on the use of oil–water interfaces saturated with lipids, which are either dissolved in the organic phase or present as liposomes supplied in the aqueous phase. One of the approaches relies on the preparation of double-emulsion droplets followed by oil removal (40, 176). Another approach, the phase-transfer method (also referred to as droplet-transfer method or method of the inverted emulsion), represents a stepwise construction of vesicles in two separate stages (140). First, one forms a water-in-oil emulsion of droplets, which will represent the GUV interior with the inner membrane leaflet. These droplets are then forced (e.g., by gravity or centrifugation) to cross an oil–water interface that is also saturated with lipids (which will constitute the outer membrane leaflet), thus forming quasi water-in-water droplets with a bilayer interface (i.e., GUVs). The droplet interface crossing may also be facilitated by capillaries (1) or planar microfluidic channels (194). These approaches allow for facile encapsulation of material inside the GUVs (132, 145), as this material can be confined in the starting water-in-oil droplets. It also allows for building GUVs with asymmetric membrane composition (140).

An alternative approach employing lipids at oil–water interfaces relies on constructing an interface between two water phases across the oil (with the dissolved lipid) and thus forming a bilayer-spanning aperture, through which a water flow is jetted to inflate GUVs (63, 184), conceptually similar to blowing soap bubbles through a ring.

GPMVs (giant plasma membrane vesicles):

vesicles derived from cells with preserved lipidome and proteome of the plasma membrane; they enable the investigation of lipid phase separation in a system with native biological complexity under physiological conditions

Proteoliposomes:

liposomes into which one or more proteins have been inserted, usually by artificial means and aided by detergents

A potential disadvantage of these methods relates to the remaining organic-phase residues in the bilayer (192) even though attempts have been made to reduce the contaminations from the oil films (89, 183). Another one is the unknown final composition of the membrane when multicomponent mixtures are employed, as lipids might have different solubility in the organic phase, as well as different partition coefficients between the interface and the organic phase (23).

2.4. More Complex Membranes, Protein Reconstitution, and Biomolecule Encapsulation

Here, we briefly introduce a couple of approaches for obtaining vesicles of higher complexity. These can be either derived from cells or established in synthetic GUVs upon (bio-) macromolecule (e.g., protein) reconstitution. Giant vesicles can also be formed by electroformation from native membrane extracts purified from cells (121), although whether the initial membrane organization and protein activity are preserved is unclear.

2.4.1. Giant plasma membrane vesicles. Giant plasma membrane vesicles (GPMVs) are also referred to as blebs and can be derived in a controlled way after subjecting cells to a cocktail of chemicals (18, 171). This approach stems from knowledge dating back to the 1960s that cultured cells shed giant vesicles from their plasma membranes upon chemical treatment (e.g., 169). The chemicals are deadly for the cells, but the resulting vesicles exhibit preserved plasma membrane lipidome and proteome (16, 104). Thus, this approach represents a poor man's way of reconstituting proteins ensuring the right conformation and orientation of the proteins, which most of the time is not as efficient in synthetic GUVs. GPMVs represent a promising system and have already proved suitable for studying phase separation in membranes, lipid-protein and lipid-lipid interactions, and adhesion (18, 189, 195, 211).

2.4.2. Protein reconstitution in synthetic giant unilamellar vesicles. A number of methods have been recently developed for the reconstitution of membrane proteins in giant vesicles. Some of them rely on the use of proteoliposomes, whereby electroformation (2, 67) or gel-assisted swelling (64, 86) can be applied to dehydrated and rehydrated films of proteoliposome. Alternatively, membrane proteins can be also directly inserted or fused to preformed lipid GUVs in physiological buffers (41). In this case, the GUVs are formed in the presence of mild detergents at subsolubilizing concentrations. This is followed either by the addition of solubilized proteins, or, alternatively, purified native vesicles or proteo-SUVs are incorporated by detergent-mediated fusion. Finally, the detergent is removed with macroporous polymeric beads.

3. PHASE STATE OF MULTICOMPONENT MEMBRANES

The quest for rafts and phase separation processes in cell membranes has been on for almost two decades, and domain formation is still a matter of ongoing debate (69, 107, 137), with a number of experimental techniques put into action (92). One important result of this search was the identification of ternary lipid mixtures that undergo phase separation into liquid-disordered and liquid-ordered phases, which can be directly observed as fluid domains in GUVs (111) using fluorescence microscopy (42) (**Figure 1**). Gel phases can also be detected typically as irregular, faceted, static domains (e.g., 13, 58, 96). Contrary to gel domains, fluid domains (in fluid environment) adopt a

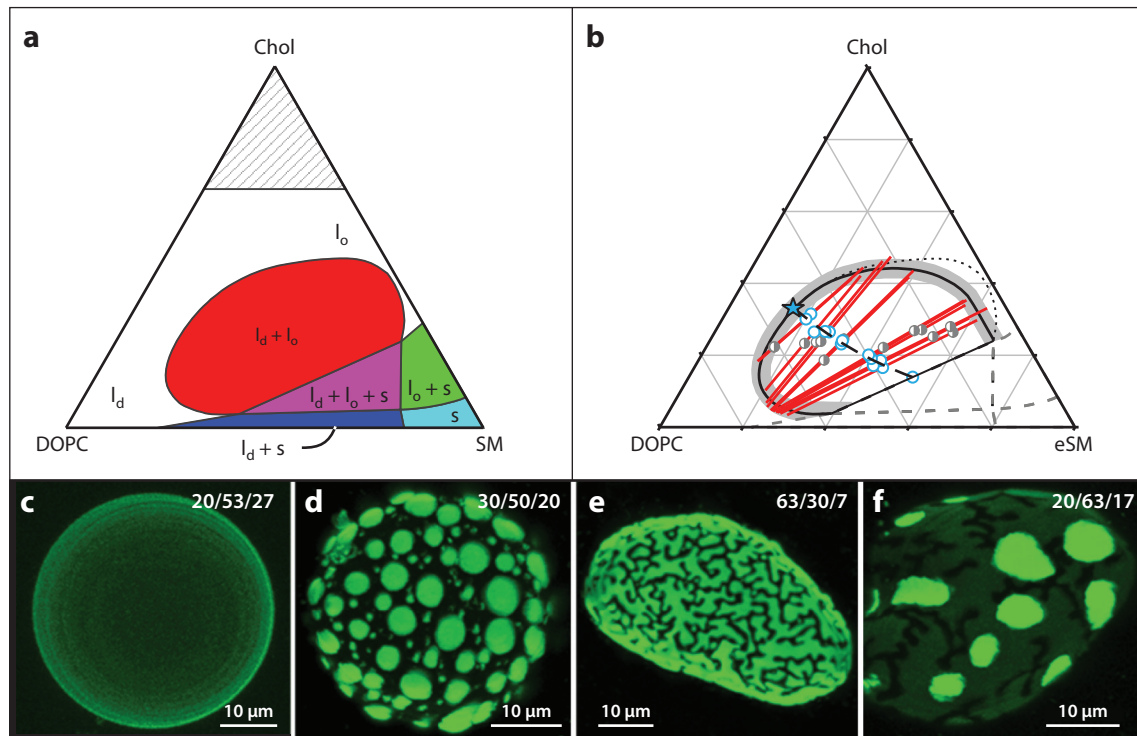


Figure 1

Phase diagrams can be deduced from fluorescence microscopy of giant vesicles. (a) Example of a phase diagram of a ternary lipid mixture of dioleoylphosphatidylcholine (DOPC), cholesterol (Chol), and sphingomyelin (SM) at $\sim 23^\circ\text{C}$, illustrating the regions of coexistence of liquid-ordered (l_o), liquid-disordered (l_d), and solid (s) phases, which have been identified predominantly from microscopy observation of giant unilamellar vesicles. (b) The phase diagram of DOPC, Chol, and egg SM (eSM) with schematically outlined regions of phase coexistence, experimentally determined tie lines (red), and the tentative critical point (star) indicated. Panels a and b adapted from Reference 20 with permission from Elsevier. Three-dimensional projections from confocal images of vesicles with (c) homogeneous membrane or exhibiting coexistence of (d) liquid-ordered and liquid-disordered, (e) liquid and solid, and (f) liquid-ordered, liquid-disordered, and solid phases; notice the partitioning of the dye (green) with preference decreasing from liquid-disordered to liquid-ordered to solid domains. The membrane composition is indicated as molar fractions (dioleoylphosphatidylglycerol/eSM/Chol) in the upper-right corners of the images. Panels c–f adapted from Reference 138 with permission from Elsevier.

circular shape to minimize line tension and may coalesce upon contact as well as bud out as first theoretically predicted in Reference 108.

3.1. Phase Diagrams

The membrane thermodynamic state is reflected in phase diagrams. They show which phases are present at certain membrane compositions and temperatures (38, 70, 198). Phase diagrams (of membranes with a limited number of components) can be obtained from fluorescence microscopy of giant vesicles. For this, a small fraction of a fluorophore (less than 1 mol%) is incorporated in the membrane preferentially partitioning in the different phases (12, 19, 93, 172) (**Figure 1c–f**). Conventional epifluorescence or confocal microscopy can be used to resolve the phase diagram (for examples of some ternary phase diagrams, see 20, 196–198, 210). Other imaging

Tie line: a line drawn in the phase coexistence region of a phase diagram of a three-component membrane; the two end points of the line meeting the binodal (which shows the boundary of the phase-coexistence region) indicate the lipid composition of the two phases for membranes with compositions located along the tie line

techniques such as fluorescence lifetime imaging microscopy have also been employed (74, 117) as has imaging with environment-sensitive dyes such as Laurdan (14).

3.2. Critical Points and Tie Lines

Giant vesicles have been used to locate important components of phase diagrams such as the critical point and tie lines. At the miscibility critical point, micron-sized compositional fluctuations can be observed, and they were found to follow two-dimensional Ising behavior both for synthetic giant vesicles (82) and for the ones derived from plasma membranes (195). Observations on GPMVs also suggested that compositions of mammalian plasma membranes are tuned to reside near a miscibility critical point. Tie lines (**Figure 1b**), and more specifically, their cross-points with the binodal, indicate the composition of domains in phase separated vesicles; the domain area fraction can be deduced using the lever rule. Tie lines are short in the immediate vicinity of the critical point (82–84, 195). Assessing them gives information about factors that drive phase separation, such as the difference in lipid acyl chain order parameters. Some examples of studies deducing tie lines from measurements on area fractions of domains in giant vesicles include References 20, 60, 87, and 196.

3.3. Factors Affecting the Phase Diagrams of Lipid Mixtures

Lipid demixing that leads to phase separation in membranes is particularly relevant to protein functionality, with activity altered depending on the local lipid environment (e.g., 88, 103). However, proteins themselves can alter the phase diagram (138). To what extent the obtained phase diagrams of lipid mixtures with only a few components are biologically relevant is still not clear, as the majority of those deduced on giant vesicles are obtained in nonphysiological buffers such as pure water, sucrose, or low-salinity solution (24, 138, 197, 199, 210). Furthermore, a recent study has shown evidence for phase separation even in quasi-single-component membranes (95). This was caused by impurities present in the used sugars (note that the typical sugar concentration used in vesicle swelling, ~ 100 mM, is orders of magnitude higher than the total lipid concentration in the sample, typically ranging from 1 to 100 μ M, which is comparable to that of impurities from sugars). Studies on charged vesicles in low-salinity buffers indicated rather small effects of salts on the membrane phase state (24, 174, 199). In contrast, neutral membranes in salt-free conditions (20) and those exposed to saline buffers in the vesicle exterior (33) seem to differ in their phase behavior. The influence of buffer composition and transmembrane solution asymmetry on the membrane phase behavior have also been recently demonstrated (97). Whether the effect of salt and solution asymmetry on the phase behavior of membranes has implications for protein adsorption and domain repartitioning remains to be seen. Membrane tension is yet another factor affecting the membrane phase state that should be considered (81, 147).

4. SOME ASSAYS FOR VESICLE MANIPULATION AND ASSESSING THE MEMBRANE MECHANICAL AND ELECTRICAL PROPERTIES

Lipid membranes are characterized by a peculiar combination of elastic properties—namely, incompressibility and very low bending rigidity. Since the pioneering work of Helfrich (77, 78), a significant number of studies have been aimed at finding ways to assess the bilayer elastic properties (e.g., 26, 44, 118, 128) and the references therein. Below, we summarize some of the most popular approaches for membrane characterization and vesicle manipulation and give a special emphasis to approaches based on the use of electric fields. One of the membrane elastic properties, the

membrane bending rigidity, is extremely sensitive to changes both in the membrane composition [even to dissolved air gas in samples (102)] and to the presence of impurities. Because of this, the bending rigidity can be employed as a control parameter when comparing different systems (44).

4.1. Fluctuation Analysis

Experimentally, fluctuation spectroscopy is probably the least demanding technique for measuring the membrane bending rigidity. It involves collecting time sequences of optical microscopy snapshots of vesicles exhibiting visible fluctuations (which implies low membrane tension). The vesicle contours are extracted (**Figure 2a**). The thermally induced fluctuations around an equilibrium shape (e.g., a sphere or a prolate) are monitored, Fourier decomposition of the contours is applied, and the mean square values of shape deviations are determined. The method has been applied to tubular vesicles (170), fractions of a vesicle (127), prolate vesicles (52), and quasispherical vesicles (72, 79, 142, 165). An exhaustive overview on the development of this method can be found in Reference 122. More recently, a new approach accounting for the finite focal depth of the microscope was reported (149), but a consensus has not yet emerged on the proposed correction.

Fluctuation analysis has been employed to resolve the effect of various molecules on the membrane rigidity, which provides a mechanistic understanding of their action in processes that they participate in. For example, depending on the membrane composition and lipid architecture, cholesterol can decrease, increase, or show no effect on the bending rigidity (72), which dethroned the traditional understanding of cholesterol as a stiffening agent observed in other GUV-based studies (55, 56, 150, 160). The activity of bulky transmembrane proteins such as bacteriorhodopsin was shown to enhance membrane fluctuations without altering the membrane rigidity (116), while other proteins and peptides were shown to reduce it (e.g., 68, 173). Salts were also reported to decrease the membrane stiffness already at millimolar concentrations (26), while the inclusion of charged lipids was found to increase the membrane stiffness. The bending rigidity is a sensitive parameter and can be affected even by the buffer type used (27).

4.2. Micropipette Aspiration and Injection

The micropipette aspiration technique was introduced by Evans, Needham, and colleagues (55–57) and ever since has been applied to characterize the elastic properties of membranes of different composition (21, 61, 80, 150, 173). The mechanical tension is generated via a suction pressure in the aspirating glass capillary (**Figure 2b**) and can be estimated from the vesicle morphology and applied pressure. In the low-tension regime, membrane undulations are pulled out and the dependence of the projected vesicle area on the tension (in logarithmic scale) yields the bending rigidity. In the high-tension regime, typically above 0.1–0.5 mN/m, the membrane is stretched (the area per lipid is increased). Here, the vesicle area scales linearly with tension, whereby the proportionality coefficient yields the stretching elasticity modulus, typically in the range of 200 to 2,000 mN/m, depending on the membrane composition and phase state (150, 151).

Micropipettes are also ubiquitously used as a manipulation technique providing a readout of the membrane tension and vesicle area (e.g., 105, 106, 191), as well as for vesicle–vesicle adhesion (54) (**Figure 2c**). Apart from holding the vesicles, micropipettes can be used to locally introduce solutions in the vesicle vicinity; even a three-pipette setup has been employed to alternate the solutions introduced around the vesicle (129). Micropipette manipulation was also recently employed in establishing a challenging system of whole-GUV patch clamping, which allowed measurement of the membrane capacitance and the activity of ion channels reconstituted in the membrane (65). Finally, sharp micropipettes (microneedles) can be employed to inject various substances such as proteins, enzymes, or DNA as aqueous solution (30) (**Figure 2d**).

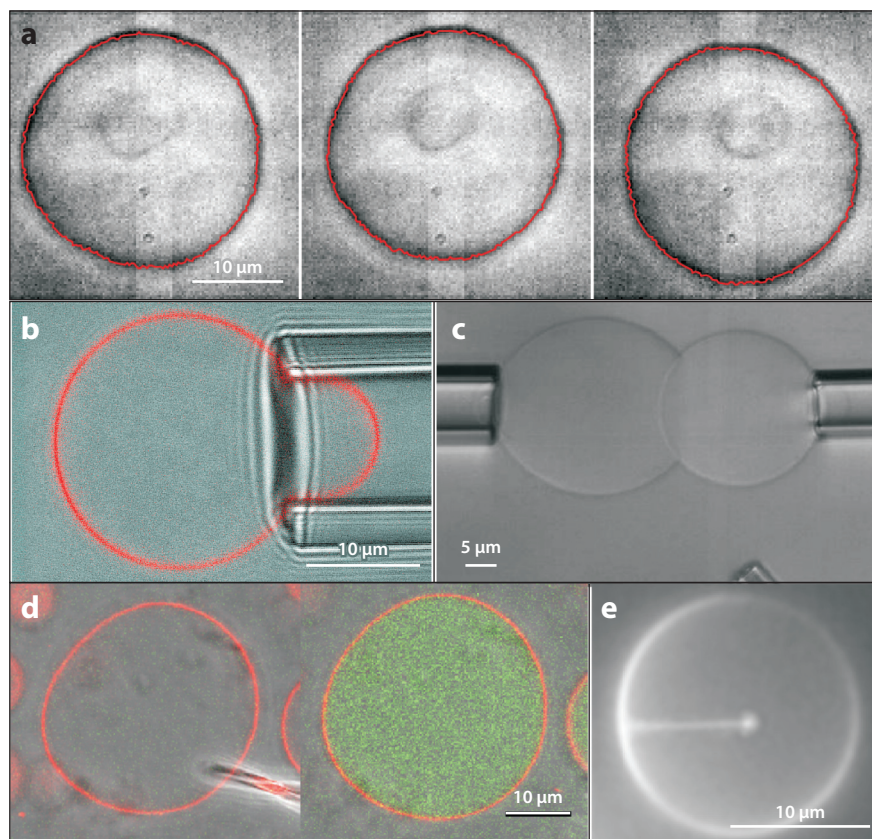
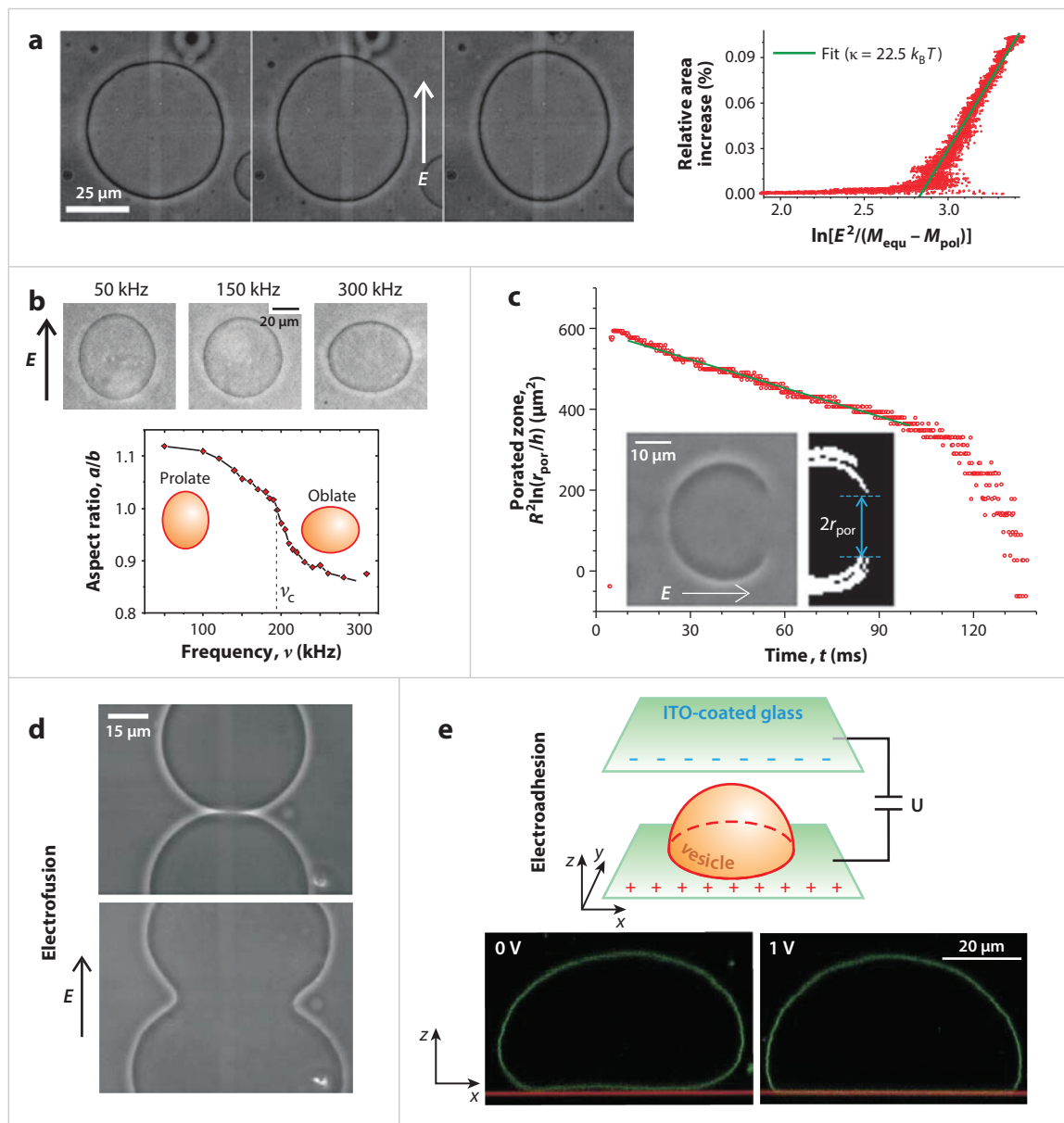


Figure 2

Techniques for assessing the membrane mechanics and for vesicle manipulation. (a) Fluctuation analysis. Phase-contrast images of a vesicle exhibiting shape fluctuations used for assessing the membrane bending rigidity. The detected vesicle contour is marked in red. The time lapse between the snapshots is several seconds. Panel *a* adapted from Reference 44 with permission from Elsevier. (b) Micropipette aspiration of a vesicle (an overlay of phase-contrast and confocal cross-section images): The membrane was fluorescently labeled (false red color). The inner diameter of the glass capillary is approximately 10 μm . Panel *b* adapted from Reference 44 with permission from Elsevier. (c) Two vesicles aspirated in micropipettes can be brought together to assess the membrane–membrane adhesion energy. Here, the adhesion is induced by a membrane–membrane bridging agent introduced via local injection through a third pipette, the tip of which is seen in the lower-right region of the snapshot. Image in panel *c* is courtesy of C. Haluska. (d) Femtoliter injection in giant unilamellar vesicles (an overlay of phase-contrast and confocal cross-section images): The vesicle (red) was immobilized on a gel substrate, and several femtoliters of a solution of low concentration of fluorescently labeled protein (green) were injected inside it. The tip of the injection pipette is seen in the lower-right corner of the left image. Images in panel *d* courtesy of Y. Avalos-Padilla. (e) In tube pulling experiments, a bead manipulated via optical tweezers is used to pull a tube out of a giant vesicle or inward as shown in this image. To pull the tube, the vesicle (i.e., the experimental chamber) is displaced relative to the position of the optical trap. Alternatively, it can be held by means of an aspiration pipette, as illustrated in Figure 4f. Panel *e* adapted from Reference 36.

4.3. Membrane Properties and Interactions Assessed from Exposing Giant Vesicles to Electric Fields

Exposing giant vesicles to electric fields offers access to versatile information about material characteristics of the membrane (46, 50). AC fields and direct current (DC) pulses can be used to deform and porate GUVs. From their response, as we briefly summarize below, one is able to deduce the membrane bending rigidity, stretching elasticity, shear surface viscosity, capacitance, and pore edge tension (**Figure 3**). Experimentally, these are undemanding measurements in terms of



(Caption appears on following page)

Figure 3 (Figure appears on preceding page)

Vesicles in electric fields: assessing membrane material properties and interactions. (a) Measuring the bending rigidity from vesicle electrodeformation at a fixed field frequency and varied field strength. From the slope of the vesicle area change as a function of electric field amplitude, E , and vesicle shape (M_{pol} and M_{equ} are the mean curvatures of the membrane at the vesicle poles and equator, respectively), one can obtain the bending rigidity. Panel *a* adapted from Reference 72 with permission from the Royal Society of Chemistry; data reproduced from Reference 62. (b) Membrane capacitance measurements. The shape response of a vesicle in a frequency sweep is used to determine the critical frequency ν_c of prolate–oblate transition, which depends solely on the membrane capacitance and the experimentally determined vesicle radius and solution conductivities. The vesicle shape is described in terms of the aspect ratio a/b of the long and short axis of the deformed vesicle. Panel *b* adapted from Reference 200 with permission from Elsevier. (c) The membrane edge tension can be estimated from the evolution of the porated region $R^2 \ln(r_{\text{por}}/b)$ as a function of time (note that to avoid plotting a dimensional value in the logarithmic term, we have introduced $b = 1 \mu\text{m}$; R is the vesicle radius). The solid line is a linear fit with slope that yields the edge tension. The inset shows a raw image (*left*) of a porated vesicle 50 ms after being exposed to an electric pulse with duration of 5 ms and amplitude of 50 kV/m. To the right is an enhanced and processed image of the vesicle half facing the cathode, showing the pore diameter, $2r_{\text{por}}$. Panel *c* adapted from Reference 146 with permission from Elsevier. (d) Fusion of two giant vesicles exposed to a direct current (DC) pulse of duration 15 μs and amplitude 3 kV/cm. The lower image shows the resulting fused vesicle 3 s after the application of the pulse. Panel *d* adapted from Reference 73, copyright 2006, National Academy of Sciences. (e) Adhesion of a giant unilamellar vesicle to a conductive substrate induced by the application of DC field of voltage U . In the absence of the field, the vesicle (*false green color*) rests on the electrode surface (*red*) and exhibits fluctuations (vertical xz confocal scans). Upon application of the field, the vesicle adheres to the substrate, exhibiting a finite contact angle. Abbreviation: ITO, indium tin oxide. Panel *e* adapted from Reference 187 with permission from Elsevier.

equipment, except if high-speed imaging is required to record fast response of the vesicles. Electric fields can be also used to manipulate vesicles, bring them together, and induce GUV–GUV fusion (**Figure 3d**). High-speed microscopy revealed that the opening of the fusion neck proceeds unprecedentedly fast (73). Adhesion of GUVs under exogenous electric field (analogous to electrowetting), whereby the adhesion strength could be smoothly regulated by turning the knob of the DC source (187), has also been explored (**Figure 3e**).

4.3.1. Measuring the membrane bending rigidity. Vesicle deformation induced by electric fields as introduced by Helfrich and coworkers (99, 130) can be used to deduce the membrane bending rigidity by subjecting a GUV to an AC electric field of increasing strength and recording the induced shape deformation (72, 99) (**Figure 3a**). The tension of the deformed vesicle is obtained from the electric stresses (for details, see 62, 72, 201, 208). Typically, the conductivity conditions in these experiments are selected so that the vesicles attain prolate deformation (9, 46) with elongation along the field direction (**Figure 3**). This method has been employed for assessing changes in the bending rigidity associated with cholesterol content (72) or presence of the ganglioside GM1 in the membrane (62). The relaxation dynamics of vesicles exposed to DC pulses can also be employed for deducing the tension and bending rigidity (209).

4.3.2. Assessing the area of floppy vesicles. Apart from measuring the membrane mechanics, vesicle electrodeformation can also be used to assess area and area changes in GUVs. Depending on the field frequency and conductivity ratio, the AC field can induce prolate and oblate deformation (9, 46). For estimating area changes, the prolate shape is preferred because of the smaller effect resulting from the proximity of the cover slip where the vesicle typically rests. Examples of the use of vesicle electrodeformation under AC fields include measurements of the area changes resulting from oxidative stress from photosensitizing molecules (154), detergent insertion (119), light-driven isomerization of molecules in the membrane (66), and vesicle fusion (113).

4.3.3. Measuring the membrane capacitance, edge tension, and viscosity. As indicated above, deformation of GUVs in electric fields can be employed for assessing the membrane

bending rigidity and vesicle area. It turns out that this undemanding experimental approach of subjecting vesicles to electric fields (both AC fields and DC pulses) can also be employed to measure a number of other material properties of the membrane. The membrane capacitance can be estimated from measuring the field frequency at which the vesicle deformation switches from prolate to oblate (162, 163, 200) (**Figure 3b**). The membrane viscosity governs the vesicle relaxation when exposed to DC pulses and can be deduced from the shape relaxation dynamics (153, 163). Strong DC pulses can induce micron-sized pores (macropores) (153), the resealing dynamics of which can be used to measure the membrane edge tension (146) (**Figure 3c**).

4.4. All-Optical Assays for Measuring the Bending Rigidity, Membrane Fluidity, and Viscosity

Assays based on contactless probing of the membrane are not limited to fluctuation spectroscopy but also include manipulation via laser beams and are demanding in terms of laboratory equipment. One example is the so-called optical stretcher where a dual-beam laser setup is used to deform GUVs and extract their elastic properties (39, 179). Another example, optical dynamometry, is based on following the sedimentation of a bead while shearing the membrane (a minimal version of a Stokes viscometer) (49). The bead is brought to and stuck to the membrane of a GUV via manipulation with optical tweezers and then released to sediment along the bilayer, yielding the membrane shear viscosity.

The category of all-optical assays includes (but is not limited to) microscopy techniques (now conventionally available in confocal microscopes), such as fluorescence recovery after photobleaching (FRAP) ubiquitously employed on GUVs to assess the membrane fluidity. Similarly (but employed to a lesser extent), fluorescence correlation spectroscopy is also used to assess association of membrane proteins and diffusion coefficients of membrane probes as well as clustering of membrane-bound molecules. Both techniques typically require immobilization of the vesicles (for an example with agarose, see 114). Finally, Förster resonance energy transfer microscopy is well established in characterizing protein binding and the degree of lipid mixing occurring via fusion (see, e.g., 113).

4.5. Pulling Membrane Tubes

Tube pulling experiments on lipid membranes produce plenty of information about the membrane characteristics, including bending rigidity, shear surface viscosity, and intermonolayer slip coefficient (36, 76). The tube diameters typically vary between 10 and 500 nm. A tube can be extruded by subjecting the vesicle to fluid drag (36, 203) or by exerting a force via a membrane-attached bead sedimenting under gravity (25), or bead manipulation with an electromagnetic field (76), a pipette (175), or optical tweezers (34); for illustration of two of these approaches, see **Figures 2e** and **4f**. Molecular motors also have been shown to be able to pull tubes out of giant vesicles (159), while micropipette manipulation has been applied to create networks of membrane tubes connecting GUVs (91). Recently, it was demonstrated that inward tubes (pointing to the vesicle interior) can also be pulled (36) (**Figure 2e**), allowing for the direct assessment of membrane spontaneous curvature (37). The tube radius can be obtained from geometrical parameters, using the conservation of membrane area and total vesicle volume.

The tube pulling technique receives increasing popularity in measurements on membranes decorated with proteins (e.g., 17, 75, 160, 180), via which dynamic processes occurring in cell membranes can be directly studied, as reviewed in Reference 158. However, the analysis should be performed with caution and the tension associated with spontaneous curvature should be carefully

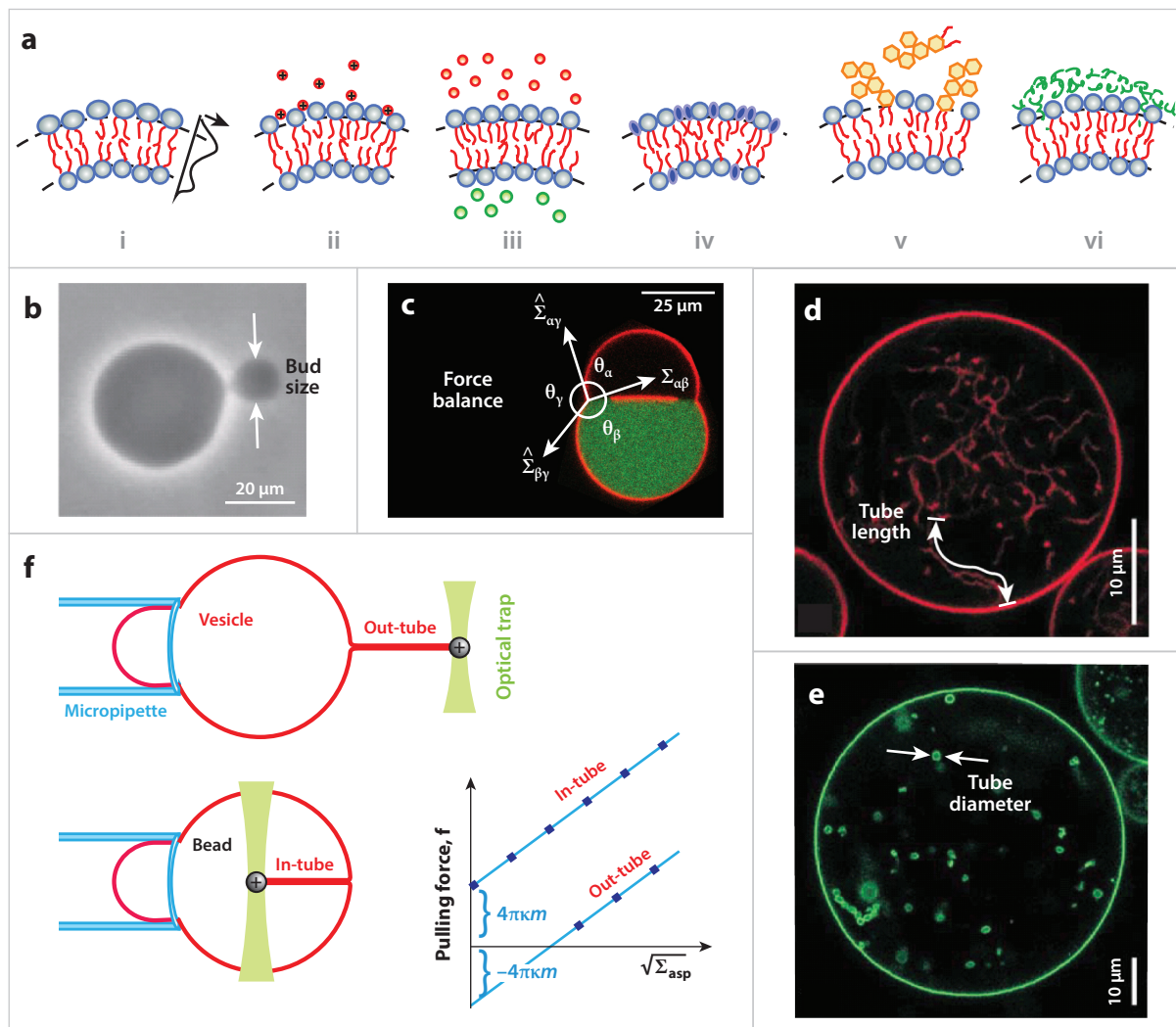
FRAP (fluorescence recovery after photobleaching): a method for measuring diffusion by observing the recovery of fluorescence in a small area or volume after photobleaching with short laser irradiation

Intermonolayer slip: describes the relative motion between the two leaflets of a bilayer; the ratio between the associated friction force per unit area and the slip velocity is known as the intermonolayer slip coefficient

considered (109). Studies based on tube pulling have demonstrated curvature-dependent sorting of lipids (160, 180) and proteins (17, 75), curvature-dependent protein binding (i.e., curvature sensing) (7, 17), fission (175), and polymerization (161) as well as curvature generation by proteins (94).

5. MEMBRANE CURVATURE AND VESICLE SHAPE

When GUVs are prepared, a number of vesicle morphologies can be observed in the sample—for example, spheres, prolates, oblates, and starfish (for a theoretical description, see 51, 110). In addition, very often, multilamellar vesicles, aggregates, and vesicles with lipid lumps are found and are typically labeled as “vesicles with defects.” In this section, we focus on the membrane spontaneous curvature, which, together with the area and volume of the vesicle, determines its shape and is a governing factor in stabilizing highly curved structures typically observed as tubes and buds.



(Caption appears on following page)

Figure 4 (Figure appears on preceding page)

Examples for sources of nonzero membrane spontaneous curvature and experimental approaches for measuring it. (a) Nonzero spontaneous curvature can be generated from (i) differences in the effective head-group size (and respective molecular area) of the lipids in the bilayer (e.g., as a result of differences in hydration, pH, or molecular type); (ii) asymmetric ion distribution, leading either to condensing or expanding the lipids in one of the bilayer leaflets; (iii) asymmetric distribution of nonadsorbing particles or (bio)molecules of different sizes; (iv) amphiphilic molecules or lipid species asymmetrically distributed in the membrane; (v) partially water-soluble molecules (such as glycolipids or peripheral proteins) asymmetrically inserting in the membrane; and (vi) asymmetrically bound proteins with specific geometry. (b) The spontaneous curvature of a budded vesicle with a closed neck can be directly assessed from its geometry following $m = (M_{\text{bud}} + M_{\text{ves}})/2$, where M_{bud} and M_{ves} are the mean curvatures of the bud and the mother vesicle, respectively (66, 131). (c) Force balance at the three-phase contact line in vesicles enclosing two aqueous phases, α and β , yields a direct dependence of the spontaneous curvature $m = -\sqrt{\frac{\Sigma_{\alpha\beta}}{2\kappa} \frac{\sin\theta_\beta}{\sin\theta_\gamma}}$ on the geometric angles, the interfacial tension $\Sigma_{\alpha\beta}$, and the membrane tensions $\hat{\Sigma}_{\alpha\gamma}$ and $\hat{\Sigma}_{\beta\gamma}$ (115). (d) The area stored in internal tubes and their length as measured from three-dimensional scans can be used to assess the tube diameter and thus the membrane spontaneous curvature (115). (e) Tube diameters can be directly measured when they are above the optical resolution. In the approaches in both panels d and e, the spontaneous curvature is $|m| = 1/R_{\text{sph}}$ for necklace tubes, where R_{sph} is the radius of the composing spheres or $|m| = 1/(2R_{\text{cyl}})$ for cylindrical tubes with radius R_{cyl} ; the sign of m is negative for inward tubes and positive for outward ones. (f) Pulling outward and inward tubes of a vesicle held by a micropipette at tension Σ_{asp} and measuring the pulling force f applied by optical tweezers yields the spontaneous curvature $= \mp \frac{f}{4\pi\kappa}$, which is determined from the y -axis intercept of force data as sketched in the inset for membranes with positive spontaneous curvature (the membrane bending rigidity κ is assessed from the slopes of the data) (37, 109). Figure adapted from Reference 15.

5.1. Spontaneous Curvature of Membranes

The asymmetry across membranes, whether resulting from differences in the leaflets compositions or from differences in the solution composition across the membrane (**Figure 4a**), gives rise to nonzero spontaneous curvature (i.e., the preferred membrane shape). In giant vesicles, nonzero membrane spontaneous curvature can be exhibited in outward or inward budding and/or tubulation. Thus, while one often looks for the “perfect” round vesicle with no inclusion and no internal or external structures, the “imperfect” GUVs may be the more representative ones (compared to the “clean” spherical vesicles), in particular for systems where the membrane and/or solution asymmetry is pronounced. Spontaneous tube formation in giant vesicles thus implies that the studied membrane exhibits spontaneous curvature, which can be positive (outward tubes/buds) or negative (inward structures). Examples of such spontaneous tubulation are provided in giant vesicles with asymmetric distribution of polyethyleneglycol in the solutions (106, 115), asymmetry in trans-leaflet distribution of the ganglioside GM1 (21, 37) or charged lipids (188), as well as protein–membrane interactions (182, 185).

5.2. Membrane Versus Monolayer Curvature

The membrane spontaneous curvature represents a material property of the membrane and should not be confused with what is sometimes referred to as molecular curvature or monolayer curvature of membrane inclusions or lipids. Indeed, the term molecular curvature is somewhat misleading, as one needs a surface to define curvature, and one molecule cannot make a surface. Even if many of the same molecule can make some type of structure (e.g., a micelle), the curvature of this shape is difficult to relate to the spontaneous curvature this molecule will generate when inserted into a membrane (see References 29 and 212 for the monolayer curvature of some lipids). This is because in the membrane, the intermolecular cohesion with the neighboring molecules is changed, and as a result, the molecule can even adopt a different geometry in space. In addition, the molecule distribution across the membrane matters. The spontaneous curvature of the membrane can change sign depending on the number of molecules in each of the leaflets, presumably irrespective of

BAR domain (Bin, amphiphysin, Rvs domain): a domain found in a large family of proteins, which forms a banana-like dimer; it differentially binds to membranes of different curvatures and tubulates lipid membranes functioning as a scaffold

the molecular shape. Spontaneous curvature of protein-doped membranes, as assessed from tube pulling experiments, are often interpreted in terms of some “effective spontaneous curvature of the protein” after taking into account its surface density (e.g., 181, p. 175). Note, however, that the obtained parameter represents, rather, a local curvature generated by the protein and is a material property that is not universal but depends on the molecule environment. Thus, reported values should not be generalized because they are characteristic for the explored system and the specific membrane composition.

To summarize, even though it is attractive to represent molecules as geometrical objects, cones, cylinders, or inverted cones, directly relating their geometry to the membrane spontaneous curvature is not straightforward unless the exact distribution across the membrane is known.

5.3. Membrane Remodeling by Proteins, Solutes, and Lipids

The membrane spontaneous curvature affects the preferred membrane shape and is therefore strongly implicated in the shape of membrane-bound organelles and cell protrusions (e.g., neurites). Indeed, the shapes of cellular organelles are highly conserved, suggesting that the morphology of their membrane is important for functionality. Membrane proteins are one of the most “popular” players considered in membrane reshaping. On the basis of their intrinsic shape [as for BAR (Bin, amphiphysin, Rvs) domains], proteins can act as curvature sensors (i.e., can bind to a membrane that is conveniently curved), but at high density, they can also induce curvature (177). Curvature effects are diverse: Both proteins and lipids can respond to curvature generation by sorting (31, 32) or can generate curvature themselves, if asymmetrically distributed across the membrane. Indeed, any type of substance, as long as it is asymmetrically distributed across a membrane, will affect the membrane spontaneous curvature. Such substances include ions (see, e.g., 90), particles, and water-soluble (macro)molecules, even those that are conventionally considered as inert to the membrane (e.g., polyethylene glycol). Only perfectly symmetric membrane leaflets and transmembrane solution compositions and asymmetric systems with perfectly balanced intermolecular interactions in both leaflets and solutions can result in a membrane of zero spontaneous curvature. This ideal case seems to be irrelevant because every biological membrane experiences asymmetry of various origins, as schematically represented in **Figure 4a**.

5.4. Measuring the Membrane Spontaneous Curvature

Knowing the membrane spontaneous curvature gives us an idea of the preferred shape the membrane will adopt when relaxed. One of the first attempts to measure the membrane spontaneous curvature, m , was applied to vesicles with sugar asymmetry across the membrane (53), yielding $m^{-1} \approx 10 \div 100 \mu\text{m}$ as assessed from the vesicle fluctuation spectra. Nonzero spontaneous curvature generation can exhibit itself in spontaneous budding or tubulation of vesicles (109) (see also **Figure 4b–e**). Several approaches for deducing m are illustrated in **Figure 4b–f**. The spontaneous curvature can vary from several inverted microns (as in the abovementioned cases) to few tens of inverted nanometers ($m^{-1} \approx 20 \div 100 \text{ nm}$), as is the case of BAR domain proteins (120). Intermediate values can be observed on membranes asymmetrically exposed to divalent ions (71) or polymers such as polyethylene glycol (115) ($m^{-1} \sim 0.1 \div 0.3 \mu\text{m}$). Measurements on systems with high spontaneous curvature typically rely on pulling lipid nanotubes out of GUVs (181) (see **Figure 4f** for one approach).

6. OUTLOOK

Giant vesicles are employed in a steeply growing number of applications, only a limited fraction of which were discussed in this review. There is no doubt that they are becoming an increasingly in-demand system, as evidenced even by the emergence of a company that provides commercial electroformation setup and a smartphone app for their production (5). How useful these enterprises are remains questionable owing to (a) the variable requirements for the encapsulated solutions, (b) the growing complexity of the membrane composition, and (c) new questions and fields addressed by means of exploiting giant vesicles.

GUVs have proved exceptionally instrumental in understanding the mechanistic action of certain proteins and peptides. A few examples include dynamin polymerization (161), Shiga toxin clustering (144, 157), the coupling of BAR domain density and membrane mechanics (177), membrane fission by protein crowding (178), curvature sorting based on steric protein interactions (182), and the membrane reshaping action of the ESCRT-III (endosomal sorting complex required for transport III) machinery (10, 207) and autophagy-related proteins (94). The mode of interaction of antimicrobial peptides with membranes has also been visualized on GUV-based assays (6).

Here, we discussed predominantly phospholipid GUVs, but studies on giant vesicles made of fatty acids have also brought understanding about processes related to the formation of protocells, such as growth of membranes, fission and fusion, and even self-reproduction of vesicles (206). Note, however, that contrary to phospholipid membranes, vesicles made of fatty acids are stable in a smaller pH range, they are more permeable, and the exchange kinetics of fatty acid molecules between the membrane and the solution as well as the flip-flop within the bilayer are faster.

As GUVs represent a simple and manageable cell-mimetic system, they are increasingly employed in synthetic biology and used in approaches toward building minimal cell- and organelle-like systems. The crowded cytoplasmic environment and ensuing phase separation were mimicked in GUVs encapsulating macromolecule solutions (47). Other examples include the establishment of a cell-free expression system encapsulated in the lumen of GUVs, where fluorescent protein expression could be followed optically (132). Because of the small volume of GUVs, substantial concentration of proteins can be reached for a short time in comparison to protein expression in bulk, where products become diluted. Limitations of current systems are outlined in Reference 100. Efforts are being made toward constructing individual modules reconstituting certain cell functionalities (168) that may lead to technological applications and pave a pathway in the far future toward building a synthetic cell (133, 155, 166, 167). Giant vesicles are already proving to be an essential component in this enterprise.

ESCRT-III (endosomal sorting complex required for transport III):

a cytosolic protein complex that remodels the membrane; as a result, the membrane bends and buds away from the compartment containing the ESCRT complex, and membrane scission follows

SUMMARY POINTS

1. Giant vesicles are becoming an increasingly in-demand system for applications in assessing material properties and interactions of biological membrane and organelle shape.
2. GUV preparation methods are constantly increasing in number, but the majority suffer from deficiencies. These should be carefully considered, depending on the target vesicle application. If the vesicles are to be used as containers, impurities in the membrane are not relevant, but if the membrane material properties are important, the presence of impurities can be crucial and the preparation method should be carefully chosen.

3. The membrane phase state can easily be influenced by environmental factors such as salinity. Thus, phase diagrams should not be considered as universal and should not be generalized.
4. Assays on GUVs for measuring membrane properties and interactions are numerous. Those based on the use of electric fields are experimentally undemanding and bring a wealth of information about the membrane elastic and electrical properties.
5. Biological membranes are asymmetric and thus characterized by a nonzero spontaneous curvature. The latter depends not only on the geometry of the constituting molecules but also on their distribution in the two leaflets.

FUTURE ISSUES

1. Increasing the complexity of the membrane of synthetic giant vesicles is still challenging and requires the development of new approaches for biomacromolecule reconstitution.
2. Preparing vesicles with size on demand using the swelling (non-oil-based) methods as well as controlled positioning of the vesicles after harvesting is still far from being established.
3. Being a simple and manageable cell-mimetic system, giant vesicles should be more intensively employed in synthetic biology applications to answer outstanding questions regarding processes like growth and division in cells and used toward building minimal cell- and organelle-like systems.

DISCLOSURE STATEMENT

The author is not aware of any affiliations, memberships, funding, or financial holdings that might be perceived as affecting the objectivity of this review.

ACKNOWLEDGMENTS

For the preparation of this review, I have profited from numerous experimental contributions and insightful discussions with skillful members of my group and current and former collaborators, including (in alphabetic order) Y. Avalos-Padilla, N. Bezlyepkina, T. Bhatia, E. Ewins, R. Dasgupta, D. Duda, H. A. Faizi, S. Frey, N. Fricke, V. N. Georgiev, M. Karimi, R. L. Knorr, B. Kubsch, R. B. Lira, S. Patarraia, K. A. Riske, T. Robinson, D. Roy, P. Salipante, P. Shchelokovskyy, J. Steinkühler, Z. Zhao, and our lab engineer C. Remde. I also wish to acknowledge the valuable insights I got from stimulating discussions with R. Lipowsky, as well as C. Marques and P. M. Vlahovska. I thank the MaxSynBio consortium, jointly funded by the Max Planck Gesellschaft and the Federal Ministry of Research, Germany, for a stimulating scientific environment. I also thank E. Ewins for proofreading the text.

LITERATURE CITED

1. Abkarian M, Loiseau E, Massiera G. 2011. Continuous droplet interface crossing encapsulation (cDICE) for high throughput monodisperse vesicle design. *Soft Matter* 7:4610–14

2. Aimon S, Manzi J, Schmidt D, Poveda Larrosa JA, Bassereau P, Toombes GES. 2011. Functional reconstitution of a voltage-gated potassium channel in giant unilamellar vesicles. *PLOS ONE* 6:e25529
3. Akashi K, Miyata H, Itoh H, Kinoshita K Jr. 1996. Preparation of giant liposomes in physiological conditions and their characterization under an optical microscope. *Biophys. J.* 71:3242–50
4. Akashi K, Miyata H, Itoh H, Kinoshita K. 1998. Formation of giant liposomes promoted by divalent cations: critical role of electrostatic repulsion. *Biophys. J.* 74:2973–82
5. Almendro Vedia VG, Natale P, Chen S, Monroy F, Rosilio V, López-Montero I. 2017. iGUVs: preparing giant unilamellar vesicles with a smartphone and lipids easily extracted from chicken eggs. *J. Chem. Educ.* 94:644–49
6. Ambroggio EE, Separovic F, Bowie JH, Fidelio GD, Bagatolli LA. 2005. Direct visualization of membrane leakage induced by the antibiotic peptides: maculatin, citropin, and aurein. *Biophys. J.* 89:1874–81
7. Ambroggio EE, Sorre B, Bassereau P, Goud B, Manneville J-B, Antonny B. 2010. ArfGAP1 generates an Arf1 gradient on continuous lipid membranes displaying flat and curved regions. *EMBO J.* 29:292–303
8. Angelova MI, Dimitrov DS. 1986. Liposome electroformation. *Faraday Discuss.* 81:303–11
9. Aranda S, Riske KA, Lipowsky R, Dimova R. 2008. Morphological transitions of vesicles induced by alternating electric fields. *Biophys. J.* 95:L19–21
10. Avalos-Padilla Y, Knorr RL, Javier-Reyna R, García-Rivera G, Lipowsky R, et al. 2018. The conserved ESCRT-III machinery participates in the phagocytosis of *Entamoeba histolytica*. *Front. Cell. Infect. Microbiol.* 8:53
11. Ayuyan AG, Cohen FS. 2006. Lipid peroxides promote large rafts: effects of excitation of probes in fluorescence microscopy and electrochemical reactions during vesicle formation. *Biophys. J.* 91:2172–83
12. Bagatolli LA. 2006. To see or not to see: lateral organization of biological membranes and fluorescence microscopy. *Biochim. Biophys. Acta Biomembr.* 1758:1541–56
13. Bagatolli LA, Gratton E. 2000. A correlation between lipid domain shape and binary phospholipid mixture composition in free standing bilayers: a two-photon fluorescence microscopy study. *Biophys. J.* 79:434–47
14. Bagatolli LA, Parasassi T, Gratton E. 2000. Giant phospholipid vesicles: comparison among the whole lipid sample characteristics using different preparation methods: a two photon fluorescence microscopy study. *Chem. Phys. Lipids* 105:135–47
15. **Bassereau P, Jin R, Baumgart T, Deserno M, Dimova R, et al. 2018. The 2018 biomembrane curvature and remodeling roadmap. *J. Phys. D Appl. Phys.* 51:343001**
16. Bauer B, Davidsson M, Orwar O. 2009. Proteomic analysis of plasma membrane vesicles. *Angew. Chem. Int. Ed.* 48:1656–59
17. Baumgart T, Capraro BR, Zhu C, Das SL. 2011. Thermodynamics and mechanics of membrane curvature generation and sensing by proteins and lipids. *Annu. Rev. Phys. Chem.* 62:483–506
18. Baumgart T, Hammond AT, Sengupta P, Hess ST, Holowka DA, et al. 2007. Large-scale fluid/fluid phase separation of proteins and lipids in giant plasma membrane vesicles. *PNAS* 104:3165–70
19. Baumgart T, Hunt G, Farkas ER, Webb WW, Feigenson GW. 2007. Fluorescence probe partitioning between L_o/L_d phases in lipid membranes. *Biochim. Biophys. Acta Biomembr.* 1768:2182–94
20. Bezlyepkina N, Gracià RS, Shchelokovskyy P, Lipowsky R, Dimova R. 2013. Phase diagram and tie-line determination for the ternary mixture DOPC/eSM/cholesterol. *Biophys. J.* 104:1456–64
21. Bhatia T, Agudo-Canalejo J, Dimova R, Lipowsky R. 2018. Membrane nanotubes increase the robustness of giant vesicles. *ACS Nano* 12:4478–85
22. Billerit C, Jeffries GDM, Orwar O, Jesorka A. 2012. Formation of giant unilamellar vesicles from spin-coated lipid films by localized IR heating. *Soft Matter* 8:10823–26
23. Blosser MC, Horst BG, Keller SL. 2016. cDICE method produces giant lipid vesicles under physiological conditions of charged lipids and ionic solutions. *Soft Matter* 12:7364–71
24. Blosser MC, Starr JB, Turtle CW, Ashcraft J, Keller SL. 2013. Minimal effect of lipid charge on membrane miscibility phase behavior in three ternary systems. *Biophys. J.* 104:2629–38
25. Bo L, Waugh RE. 1989. Determination of bilayer-membrane bending stiffness by tether formation from giant, thin-walled vesicles. *Biophys. J.* 55:509–17
15. A collection of short review contributions aiming at the mechanistic understanding and quantification of membrane remodeling, outlining current and future challenges in the field.

26. Bouvrais H. 2012. Bending rigidities of lipid bilayers: their determination and main inputs in biophysical studies. *Adv. Planar Lipid Bilayers Liposomes* 15:1–75
27. Bouvrais H, Duelund L, Ipsen JH. 2014. Buffers affect the bending rigidity of model lipid membranes. *Langmuir* 30:13–16
28. Breton M, Amirkavei M, Mir LM. 2015. Optimization of the electroformation of giant unilamellar vesicles (GUVs) with unsaturated phospholipids. *J. Membr. Biol.* 248:827–35
29. Brown MF. 2017. Soft matter in lipid–protein interactions. *Annu. Rev. Biophys.* 46:379–410
30. Bucher P, Fischer A, Luisi PL, Oberholzer T, Walde P. 1998. Giant vesicles as biochemical compartments: the use of microinjection techniques. *Langmuir* 14:2712–21
31. Callan-Jones A, Bassereau P. 2013. Curvature-driven membrane lipid and protein distribution. *Curr. Opin. Solid State Mater. Sci.* 17:143–50
32. Callan-Jones A, Sorre B, Bassereau P. 2011. Curvature-driven lipid sorting in biomembranes. *Cold Spring Harb. Perspect. Biol.* 3:a004648
33. Carravilla P, Nieva JL, Goñi FM, Requejo-Isidro J, Huarte N. 2015. Two-photon Laurdan studies of the ternary lipid mixture DOPC:SM:cholesterol reveal a single liquid phase at sphingomyelin:cholesterol ratios lower than 1. *Langmuir* 31:2808–17
34. Cuvelier D, Derenyi I, Bassereau P, Nassoy P. 2005. Coalescence of membrane tethers: experiments, theory, and applications. *Biophys. J.* 88:2714–26
35. Dao TPT, Fauquignon M, Fernandes F, Ibarboure E, Vax A, et al. 2017. Membrane properties of giant polymer and lipid vesicles obtained by electroformation and PVA gel-assisted hydration methods. *Colloids Surf. A Physicochem. Eng. Aspects* 533:347–53
36. Dasgupta R, Dimova R. 2014. Inward and outward membrane tubes pulled from giant vesicles. *J. Phys. D Appl. Phys.* 47:282001
37. Dasgupta R, Miettinen MS, Fricke N, Lipowsky R, Dimova R. 2018. The glycolipid GM1 reshapes asymmetric biomembranes and giant vesicles by curvature generation. *PNAS* 115:5756–61
38. de Almeida RFM, Fedorov A, Prieto M. 2003. Sphingomyelin/phosphatidylcholine/cholesterol phase diagram: boundaries and composition of lipid rafts. *Biophys. J.* 85:2406–16
39. Delabre U, Feld K, Crespo E, Whyte G, Sykes C, et al. 2015. Deformation of phospholipid vesicles in an optical stretcher. *Soft Matter* 11:6075–88
40. Deng N-N, Yelleswarapu M, Huck WTS. 2016. Monodisperse uni- and multicompartment liposomes. *J. Am. Chem. Soc.* 138:7584–91
41. Dezi M, Di Cicco A, Bassereau P, Lévy D. 2013. Detergent-mediated incorporation of transmembrane proteins in giant unilamellar vesicles with controlled physiological contents. *PNAS* 110:7276–81
42. Dietrich C, Bagatolli LA, Volovyk ZN, Thompson NL, Levi M, et al. 2001. Lipid rafts reconstituted in model membranes. *Biophys. J.* 80:1417–28
43. Dimova R. 2012. Giant vesicles: a biomimetic tool for membrane characterization. *Adv. Planar Lipid Bilayers Liposomes* 16:1–50
44. **Dimova R. 2014. Recent developments in the field of bending rigidity measurements on membranes. *Adv. Colloid Interface Sci.* 208:225–34**
45. Dimova R, Aranda S, Bezlyepkina N, Nikolov V, Riske KA, Lipowsky R. 2006. A practical guide to giant vesicles. Probing the membrane nanoregime via optical microscopy. *J. Phys. Condens. Matter* 18:S1151–76
46. Dimova R, Bezlyepkina N, Jordo MD, Knorr RL, Riske KA, et al. 2009. Vesicles in electric fields: some novel aspects of membrane behavior. *Soft Matter* 5:3201–12
47. Dimova R, Lipowsky R. 2017. Giant vesicles exposed to aqueous two-phase systems: membrane wetting, budding processes, and spontaneous tubulation. *Adv. Mater. Interfaces* 4:1600451
48. Dimova R, Marques C. 2019. *The Giant Vesicle Book*. Boca Raton, FL: Taylor & Francis Group
49. Dimova R, Pouligny B, Dietrich C. 2000. Pretransitional effects in dimyristoylphosphatidylcholine vesicle membranes: optical dynamometry study. *Biophys. J.* 79:340–56
50. Dimova R, Riske KA, Aranda S, Bezlyepkina N, Knorr RL, Lipowsky R. 2007. Giant vesicles in electric fields. *Soft Matter* 3:817–27
51. Dobereiner HG. 2000. Properties of giant vesicles. *Curr. Opin. Colloid Interface Sci.* 5:256–63

44. Provides a survey on methods for assessing the membrane bending rigidity and factors influencing it.

52. Dobreiner HG, Gompper G, Haluska CK, Kroll DM, Petrov PG, Riske KA. 2003. Advanced flicker spectroscopy of fluid membranes. *Phys. Rev. Lett.* 91:4
53. Dobreiner HG, Selchow O, Lipowsky R. 1999. Spontaneous curvature of fluid vesicles induced by trans-bilayer sugar asymmetry. *Eur. Biophys. J. Biophys. Lett.* 28:174–78
54. Evans E, Metcalfe M. 1984. Free-energy potential for aggregation of giant, neutral lipid bilayer vesicles by Van der Waals attraction. *Biophys. J.* 46:423–26
55. Evans E, Needham D. 1987. Physical properties of surfactant bilayer membranes: thermal transitions, elasticity, rigidity, cohesion, and colloidal interactions. *J. Phys. Chem.* 91:4219–28
56. Evans E, Rawicz W. 1990. Entropy-driven tension and bending elasticity in condensed-fluid membranes. *Phys. Rev. Lett.* 64:2094–97
57. Evans EA. 1983. Bending elastic-modulus of red-blood-cell membrane derived from buckling instability in micropipet aspiration tests. *Biophys. J.* 43:27–30
58. Feigenson GW, Buboltz JT. 2001. Ternary phase diagram of dipalmitoyl-PC/dilauroyl-PC/cholesterol: nanoscopic domain formation driven by cholesterol. *Biophys. J.* 80:2775–88
59. Fenz SF, Sengupta K. 2012. Giant vesicles as cell models. *Integr. Biol.* 4:982–95
60. Fidorra M, Garcia A, Ipsen JH, Hartel S, Bagatolli LA. 2009. Lipid domains in giant unilamellar vesicles and their correspondence with equilibrium thermodynamic phases: a quantitative fluorescence microscopy imaging approach. *Biochim. Biophys. Acta Biomembr.* 1788:2142–49
61. Fournier JB, Ajdari A, Peliti L. 2001. Effective-area elasticity and tension of micromanipulated membranes. *Phys. Rev. Lett.* 86:4970–73
62. Fricke N, Dimova R. 2016. GM1 softens POPC membranes and induces the formation of micron-sized domains. *Biophys. J.* 111:1935–45
63. Funakoshi K, Suzuki H, Takeuchi S. 2007. Formation of giant lipid vesiclelike compartments from a planar lipid membrane by a pulsed jet flow. *J. Am. Chem. Soc.* 129:12608–9
64. Garten M, Aimon S, Bassereau P, Toombes GES. 2015. Reconstitution of a transmembrane protein, the voltage-gated ion channel, KvAP, into giant unilamellar vesicles for microscopy and patch clamp studies. *J. Vis. Exp.* 95:e52281
65. Garten M, Mosgaard LD, Bornschlöggl T, Dieudonné S, Bassereau P, Toombes GES. 2017. Whole-GUV patch-clamping. *PNAS* 114:328
66. Georgiev VN, Grafmüller A, Bléger D, Hecht S, Kunstmann S, et al. 2018. Area increase and budding in giant vesicles triggered by light: behind the scene. *Adv. Sci.* 5:1800432
67. Girard P, Pécéréaux J, Lenoir G, Falson P, Rigaud J-L, Bassereau P. 2004. A new method for the reconstitution of membrane proteins into giant unilamellar vesicles. *Biophys. J.* 87:419–29
68. Girard P, Prost J, Bassereau P. 2005. Passive or active fluctuations in membranes containing proteins. *Phys. Rev. Lett.* 94:088102
69. Goñi FM. 2014. The basic structure and dynamics of cell membranes: an update of the Singer-Nicolson model. *Biochim. Biophys. Acta Biomembr.* 1838:1467–76
70. Goñi FM, Alonso A, Bagatolli LA, Brown RE, Marsh D, et al. 2008. Phase diagrams of lipid mixtures relevant to the study of membrane rafts. *Biochim. Biophys. Acta Mol. Cell Biol. Lipids* 1781:665–84
71. Graber ZT, Shi Z, Baumgart T. 2017. Cations induce shape remodeling of negatively charged phospholipid membranes. *Phys. Chem. Chem. Phys.* 19:15285–95
72. Gracià RS, Bezlyepkina N, Knorr RL, Lipowsky R, Dimova R. 2010. Effect of cholesterol on the rigidity of saturated and unsaturated membranes: fluctuation and electrodeformation analysis of giant vesicles. *Soft Matter* 6:1472–82
73. Haluska CK, Riske KA, Marchi-Artzner V, Lehn JM, Lipowsky R, Dimova R. 2006. Time scales of membrane fusion revealed by direct imaging of vesicle fusion with high temporal resolution. *PNAS* 103:15841–46
74. Haluska CK, Schroder AP, Didier P, Heissler D, Duportail G, et al. 2008. Combining fluorescence lifetime and polarization microscopy to discriminate phase separated domains in giant unilamellar vesicles. *Biophys. J.* 95:5737–47
75. Heinrich M, Tian A, Esposito C, Baumgart T. 2010. Dynamic sorting of lipids and proteins in membrane tubes with a moving phase boundary. *PNAS* 107:7208–13

77. Seminal paper that introduces the concepts of membrane bending elasticity and spontaneous curvature.

76. Heinrich V, Waugh RE. 1996. A piconewton force transducer and its application to measurement of the bending stiffness of phospholipid membranes. *Ann. Biomed. Eng.* 24:595–605
77. Helfrich W. 1973. Elastic properties of lipid bilayers: theory and possible experiments. *Z. Naturforsch.* 28:693–703
78. Helfrich W. 1974. Blocked lipid exchange in bilayers and its possible influence on shape of vesicles. *Z. Naturforsch.* 29:510–15
79. Henriksen J, Rowat AC, Ipsen JH. 2004. Vesicle fluctuation analysis of the effects of sterols on membrane bending rigidity. *Eur. Biophys. J. Biophys. Lett.* 33:732–41
80. Henriksen JR, Ipsen JH. 2004. Measurement of membrane elasticity by micro-pipette aspiration. *Eur. Phys. J. E* 14:149–67
81. Ho JCS, Rangamani P, Liedberg B, Parikh AN. 2016. Mixing water, transducing energy, and shaping membranes: autonomously self-regulating giant vesicles. *Langmuir* 32:2151–63
82. Honerkamp-Smith AR, Cicuta P, Collins MD, Veatch SL, den Nijs M, et al. 2008. Line tensions, correlation lengths, and critical exponents in lipid membranes near critical points. *Biophys. J.* 95:236–46
83. Honerkamp-Smith AR, Machta BB, Keller SL. 2012. Experimental observations of dynamic critical phenomena in a lipid membrane. *Phys. Rev. Lett.* 108:265702
84. Honerkamp-Smith AR, Veatch SL, Keller SL. 2009. An introduction to critical points for biophysicists; observations of compositional heterogeneity in lipid membranes. *Biochim. Biophys. Acta Biomembr.* 1788:53–63
85. Horger KS, Estes DJ, Capone R, Mayer M. 2009. Films of agarose enable rapid formation of giant liposomes in solutions of physiologic ionic strength. *J. Am. Chem. Soc.* 131:1810–19
86. Horger KS, Liu H, Rao DK, Shukla S, Sept D, et al. 2015. Hydrogel-assisted functional reconstitution of human P-glycoprotein (ABCB1) in giant liposomes. *Biochim. Biophys. Acta* 1848:643–53
87. Husen P, Arriaga LR, Monroy F, Ipsen JH, Bagatolli LA. 2012. Morphometric image analysis of giant vesicles: a new tool for quantitative thermodynamics studies of phase separation in lipid membranes. *Biophys. J.* 103:2304–10
88. Kahya N, Brown DA, Schwille P. 2005. Raft partitioning and dynamic behavior of human placental alkaline phosphatase in giant unilamellar vesicles. *Biochemistry* 44:7479–89
89. Karamdad K, Law RV, Seddon JM, Brooks NJ, Ces O. 2015. Preparation and mechanical characterisation of giant unilamellar vesicles by a microfluidic method. *Lab Chip* 15:557–62
90. Karimi M, Steinkühler J, Roy D, Dasgupta R, Lipowsky R, Dimova R. 2018. Asymmetric ionic conditions generate large membrane curvatures. *Nano Lett.* 18(12):7816–21
91. Karlsson M, Sott K, Cans AS, Karlsson A, Karlsson R, Orwar O. 2001. Micropipet-assisted formation of microscopic networks of unilamellar lipid bilayer nanotubes and containers. *Langmuir* 17:6754–58
92. Klotzsch E, Schutz GJ. 2013. A critical survey of methods to detect plasma membrane rafts. *Philos. Trans. R. Soc. B* 368:20120033
93. Klymchenko AS, Kreder R. 2014. Fluorescent probes for lipid rafts: from model membranes to living cells. *Chem. Biol.* 21:97–113
94. Knorr RL, Nakatogawa H, Ohsumi Y, Lipowsky R, Baumgart T, Dimova R. 2014. Membrane morphology is actively transformed by covalent binding of the protein Atg8 to PE-lipids. *PLOS ONE* 9:e115357
95. Knorr RL, Steinkühler J, Dimova R. 2018. Micron-sized domains in quasi single-component giant vesicles. *Biochim. Biophys. Acta Biomembr.* 1860:1957–64
96. Korlach J, Schwille P, Webb WW, Feigenson GW. 1999. Characterization of lipid bilayer phases by confocal microscopy and fluorescence correlation spectroscopy. *PNAS* 96:8461–66
97. Kubsch B, Robinson T, Lipowsky R, Dimova R. 2016. Solution asymmetry and salt expand fluid-fluid coexistence regions of charged membranes. *Biophys. J.* 110:2581–84
98. Kubsch B, Robinson T, Steinkühler J, Dimova R. 2017. Phase behavior of charged vesicles under symmetric and asymmetric solution conditions monitored with fluorescence microscopy. *J. Vis. Exp.* 128:e56034
99. Kummrow M, Helfrich W. 1991. Deformation of giant lipid vesicles by electric-fields. *Phys. Rev. A* 44:8356–60

100. Lagny TJ, Bassereau P. 2015. Bioinspired membrane-based systems for a physical approach of cell organization and dynamics: usefulness and limitations. *Interface Focus* 5:20150038
101. Le Berre M, Yamada A, Reck L, Chen Y, Baigl D. 2008. Electroformation of giant phospholipid vesicles on a silicon substrate: advantages of controllable surface properties. *Langmuir* 24:2643–49
102. Lee C-W, Chiang Y-L, Liu J-T, Chen Y-X, Lee C-H, et al. 2018. Emerging roles of air gases in lipid bilayers. *Small* 14. <https://doi.org/10.1002/sml.201802133>
103. Levental I, Grzybek M, Simons K. 2010. Greasing their way: lipid modifications determine protein association with membrane rafts. *Biochemistry* 49:6305–16
104. Levental I, Veatch SL. 2016. The continuing mystery of lipid rafts. *J. Mol. Biol.* 428:4749–64
105. Li NW, Sharifi-Mood N, Tu FQ, Lee D, Radhakrishnan R, et al. 2017. Curvature-driven migration of colloids on tense lipid bilayers. *Langmuir* 33:600–10
106. Li Y, Lipowsky R, Dimova R. 2011. Membrane nanotubes induced by aqueous phase separation and stabilized by spontaneous curvature. *PNAS* 108:4731–36
107. Lingwood D, Simons K. 2010. Lipid rafts as a membrane-organizing principle. *Science* 327:46–50
108. Lipowsky R. 1992. Budding of membranes induced by intramembrane domains. *J. Phys. II* 2:1825–40
109. Lipowsky R. 2013. Spontaneous tubulation of membranes and vesicles reveals membrane tension generated by spontaneous curvature. *Faraday Discuss.* 161:305–31
110. Lipowsky R. 2014. Coupling of bending and stretching deformations in vesicle membranes. *Adv. Colloid Interface Sci.* 208:14–24
111. Lipowsky R, Dimova R. 2003. Domains in membranes and vesicles. *J. Phys. Condens. Matter* 15:S31–45
112. Lira RB, Dimova R, Riske KA. 2014. Giant unilamellar vesicles formed by hybrid films of agarose and lipids display altered mechanical properties. *Biophys. J.* 107:1609–19
113. Lira RB, Robinson T, Dimova R, Riske KA. 2019. Highly efficient protein-free membrane fusion: a giant vesicle study. *Biophys. J.* 116(1):79–91
114. Lira RB, Steinkühler J, Knorr RL, Dimova R, Riske KA. 2016. Posing for a picture: vesicle immobilization in agarose gel. *Sci. Rep.* 6:25254
115. Liu Y, Agudo-Canalejo J, Grafmüller A, Dimova R, Lipowsky R. 2016. Patterns of flexible nanotubes formed by liquid-ordered and liquid-disordered membranes. *ACS Nano* 10:463–74
116. Manneville JB, Bassereau P, Levy D, Prost J. 1999. Activity of transmembrane proteins induces magnification of shape fluctuations of lipid membranes. *Phys. Rev. Lett.* 82:4356–59
117. Margineanu A, Hotta J-I, Van der Auweraer M, Ameloot M, Stefan A, et al. 2007. Visualization of membrane rafts using a perylene monoimide derivative and fluorescence lifetime imaging. *Biophys. J.* 93:2877–91
118. Marsh D. 2006. Elastic curvature constants of lipid monolayers and bilayers. *Chem. Phys. Lipids* 144:146–59
119. Mattei B, Franca ADC, Riske KA. 2015. Solubilization of binary lipid mixtures by the detergent Triton X-100: the role of cholesterol. *Langmuir* 31:378–86
120. McMahon HT, Gallop JL. 2005. Membrane curvature and mechanisms of dynamic cell membrane remodelling. *Nature* 438:590–96
121. Méléard P, Bagatolli LA, Pott T. 2009. Giant unilamellar vesicle electroformation: from lipid mixtures to native membranes under physiological conditions. *Methods Enzymol.* 465:161–76
122. Méléard P, Pott T. 2013. Overview of a quest for bending elasticity measurement. *Adv. Planar Lipid Bilayers Liposomes* 17:55–75
123. Menger FM, Keiper JS. 1998. Chemistry and physics of giant vesicles as biomembrane models. *Curr. Opin. Chem. Biol.* 2:726–32
124. Montes LR, Alonso A, Goñi FM, Bagatolli LA. 2007. Giant unilamellar vesicles electroformed from native membranes and organic lipid mixtures under physiological conditions. *Biophys. J.* 93:3548–54
125. Mora NL, Hansen JS, Gao Y, Ronald AA, Kieleyka R, et al. 2014. Preparation of size tunable giant vesicles from cross-linked dextran(ethylene glycol) hydrogels. *Chem. Commun.* 50:1953–55
126. Morales-Pennington NF, Wu J, Farkas ER, Goh SL, Konyakhina TM, et al. 2010. GUV preparation and imaging: Minimizing artifacts. *Biochim. Biophys. Acta* 1798:1324–32

103. Reviews how protein activities can be affected by the local lipid composition of the membrane.

104. Discusses giant plasma membrane vesicles, how closely they represent the plasma membrane lipidome and proteome, and their use in characterizing raft formation and behavior.

133 and 166. Provide insights into what should be achieved to set up rudimentary synthetic organisms inspired by biology.

127. Mutz M, Helfrich W. 1990. Bending rigidities of some biological model membranes as obtained from the Fourier-analysis of contour sections. *J. Phys.* 51:991–1002
128. Nagle JF. 2013. Introductory lecture: basic quantities in model biomembranes. *Faraday Discuss.* 161:11–29
129. Needham D, Stoiicheva N, Zhelev DV. 1997. Exchange of monooleoylphosphatidylcholine as monomer and micelle with membranes containing poly(ethylene glycol)-lipid. *Biophys. J.* 73:2615–29
130. Niggemann G, Kummrow M, Helfrich W. 1995. The bending rigidity of phosphatidylcholine bilayers: dependences on experimental method, sample cell sealing and temperature. *J. Phys. II* 5:413–25
131. Nikolov V, Lipowsky R, Dimova R. 2007. Behavior of giant vesicles with anchored DNA molecules. *Biophys. J.* 92:4356–68
132. Noireaux V, Libchaber A. 2004. A vesicle bioreactor as a step toward an artificial cell assembly. *PNAS* 101:17669–74
133. **Noireaux V, Maeda YT, Libchaber A. 2011. Development of an artificial cell, from self-organization to computation and self-reproduction. *PNAS* 108:3473**
134. Nourian Z, Roelofsen W, Danelon C. 2012. Triggered gene expression in fed-vesicle microreactors with a multifunctional membrane. *Angew. Chem. Int. Ed.* 51:3114–18
135. Oku N, MacDonald RC. 1983. Differential effects of alkali metal chlorides on formation of giant liposomes by freezing and thawing and by dialysis. *Biochemistry* 22:855–63
136. Okumura Y, Zhang H, Sugiyama T, Iwata Y. 2007. Electroformation of giant vesicles on a non-electroconductive substrate. *J. Am. Chem. Soc.* 129:1490–91
137. Owen DM, Magenau A, Williamson D, Gaus K. 2012. The lipid raft hypothesis revisited—new insights on raft composition and function from super-resolution fluorescence microscopy. *BioEssays* 34:739–47
138. Patarala S, Liu YG, Lipowsky R, Dimova R. 2014. Effect of cytochrome c on the phase behavior of charged multicomponent lipid membranes. *Biochim. Biophys. Acta Biomembr.* 1838:2036–45
139. Patil YP, Jadhav S. 2014. Novel methods for liposome preparation. *Chem. Phys. Lipids* 177:8–18
140. Pautot S, Frisken BJ, Weitz DA. 2003. Engineering asymmetric vesicles. *PNAS* 100:10718
141. Pavlič JI, Genova J, Popkirov G, Kralj-Iglič V, Iglič A, Mitov MD. 2011. Mechanoformation of neutral giant phospholipid vesicles in high ionic strength solution. *Chem. Phys. Lipids* 164:727–31
142. Pecreaux J, Dohereiner HG, Prost J, Joanny JF, Bassereau P. 2004. Refined contour analysis of giant unilamellar vesicles. *Eur. Phys. J. E* 13:277–90
143. Pereno V, Carugo D, Bau L, Sezgin E, Bernardino de la Serna J, et al. 2017. Electroformation of giant unilamellar vesicles on stainless steel electrodes. *ACS Omega* 2:994–1002
144. Pezeshkian W, Gao H, Arumugam S, Becken U, Bassereau P, et al. 2017. Mechanism of Shiga toxin clustering on membranes. *ACS Nano* 11:314–24
145. Pontani L-L, van der Gucht J, Salbreux G, Heuvingh J, Joanny J-F, Sykes C. 2009. Reconstitution of an actin cortex inside a liposome. *Biophys. J.* 96:192–98
146. Portet T, Dimova R. 2010. A new method for measuring edge tensions and stability of lipid bilayers: effect of membrane composition. *Biophys. J.* 99:3264–73
147. Portet T, Gordon SE, Keller SL. 2012. Increasing membrane tension decreases miscibility temperatures; an experimental demonstration via micropipette aspiration. *Biophys. J.* 103:L35–37
148. Pott T, Bouvrain H, Méléard P. 2008. Giant unilamellar vesicle formation under physiologically relevant conditions. *Chem. Phys. Lipids* 154:115–19
149. Rautu SA, Orsi D, Di Michele L, Rowlands G, Cicuta P, Turner MS. 2017. The role of optical projection in the analysis of membrane fluctuations. *Soft Matter* 13:3480–83
150. Rawicz W, Olbrich KC, McIntosh T, Needham D, Evans E. 2000. Effect of chain length and unsaturation on elasticity of lipid bilayers. *Biophys. J.* 79:328–39
151. Rawicz W, Smith BA, McIntosh TJ, Simon SA, Evans E. 2008. Elasticity, strength, and water permeability of bilayers that contain raft microdomain-forming lipids. *Biophys. J.* 94:4725–36
152. Reeves JP, Dowben RM. 1969. Formation and properties of thin-walled phospholipid vesicles. *J. Cell. Physiol.* 73:49–60
153. Riske KA, Dimova R. 2005. Electro-deformation and poration of giant vesicles viewed with high temporal resolution. *Biophys. J.* 88:1143–55

154. Riske KA, Sudbrack TP, Archilha NL, Uchoa AF, Schroder AP, et al. 2009. Giant vesicles under oxidative stress induced by a membrane-anchored photosensitizer. *Biophys. J.* 97:1362–70
155. Robinson T, Verboket PE, Eyer K, Dittrich PS. 2014. Controllable electrofusion of lipid vesicles: initiation and analysis of reactions within biomimetic containers. *Lab Chip* 14:2852–59
156. Rodriguez N, Pincet F, Cribier S. 2005. Giant vesicles formed by gentle hydration and electroformation: A comparison by fluorescence microscopy. *Colloids Surf. B Biointerfaces* 42:125–30
157. Römer W, Berland L, Chambon V, Gaus K, Windschiegl B, et al. 2007. Shiga toxin induces tubular membrane invaginations for its uptake into cells. *Nature* 450:670–75
- 158. Roux A. 2013. The physics of membrane tubes: soft templates for studying cellular membranes. *Soft Matter* 9:6726–36**
159. Roux A, Cappello G, Cartaud J, Prost J, Goud B, Bassereau P. 2002. A minimal system allowing tubulation with molecular motors pulling on giant liposomes. *PNAS* 99:5394–99
160. Roux A, Cuvelier D, Nassoy P, Prost J, Bassereau P, Goud B. 2005. Role of curvature and phase transition in lipid sorting and fission of membrane tubules. *EMBO J.* 24:1537–45
161. Roux A, Koster G, Lenz M, Sorre B, Manneville JB, et al. 2010. Membrane curvature controls dynamin polymerization. *PNAS* 107:4141–46
162. Salipante PF, Knorr RL, Dimova R, Vlahovska PM. 2012. Electrodeformation method for measuring the capacitance of bilayer membranes. *Soft Matter* 8:3810–16
163. Salipante PF, Vlahovska PM. 2014. Vesicle deformation in DC electric pulses. *Soft Matter* 10:3386–93
164. Schmid EM, Richmond DL, Fletcher DA. 2015. Reconstitution of proteins on electroformed giant unilamellar vesicles. *Methods Cell Biol.* 128:319–38
165. Schneider MB, Jenkins JT, Webb WW. 1984. Thermal fluctuations of large quasi-spherical bimolecular phospholipid-vesicles. *J. Phys.* 45:1457–72
- 166. Schwille P. 2011. Bottom-up synthetic biology: engineering in a tinkerer's world. *Science* 333:1252**
167. Schwille P, Diez S. 2009. Synthetic biology of minimal systems. *Crit. Rev. Biochem. Mol. Biol.* 44:223–42
168. Schwille P, Spatz J, Landfester K, Bodenschatz E, Herminghaus S, et al. 2018. MaxSynBio: avenues towards creating cells from the bottom up. *Angew. Chem. Int. Ed.* 57:13382–92
169. Scott RE. 1976. Plasma membrane vesiculation: a new technique for isolation of plasma membranes. *Science* 194:743
170. Servuss RM, Harbich W, Helfrich W. 1976. Measurement of curvature-elastic modulus of egg lecithin bilayers. *Biochim. Biophys. Acta* 436:900–3
171. Sezgin E, Kaiser HJ, Baumgart T, Schwille P, Simons K, Levental I. 2012. Elucidating membrane structure and protein behavior using giant plasma membrane vesicles. *Nat. Protoc.* 7:1042–51
172. Sezgin E, Sadowski T, Simons K. 2014. Measuring lipid packing of model and cellular membranes with environment sensitive probes. *Langmuir* 30:8160–66
173. Shchelokovskyy P, Tristram-Nagle S, Dimova R. 2011. Effect of the HIV-1 fusion peptide on the mechanical properties and leaflet coupling of lipid bilayers. *New J. Phys.* 13:025004
174. Shimokawa N, Hishida M, Seto H, Yoshikawa K. 2010. Phase separation of a mixture of charged and neutral lipids on a giant vesicle induced by small cations. *Chem. Phys. Lett.* 496:59–63
175. Shnyrova AV, Bashkirov PV, Akimov SA, Pucadyil TJ, Zimmerberg J, et al. 2013. Geometric catalysis of membrane fission driven by flexible dynamin rings. *Science* 339:1433–36
176. Shum HC, Lee D, Yoon I, Kodger T, Weitz DA. 2008. Double emulsion templated monodisperse phospholipid vesicles. *Langmuir* 24:7651–53
177. Simunovic M, Voth GA, Callan-Jones A, Bassereau P. 2015. When physics takes over: BAR proteins and membrane curvature. *Trends Cell Biol.* 25:780–92
178. Snead WT, Hayden CC, Gadok AK, Zhao C, Lafer EM, et al. 2017. Membrane fission by protein crowding. *PNAS* 114:E3258
179. Solmaz ME, Sankhagowit S, Biswas R, Mejia CA, Povinelli ML, Malmstadt N. 2013. Optical stretching as a tool to investigate the mechanical properties of lipid bilayers. *RSC Adv.* 3:16632–38
- 180. Sorre B, Callan-Jones A, Manneville JB, Nassoy P, Joanny JF, et al. 2009. Curvature-driven lipid sorting needs proximity to a demixing point and is aided by proteins. *PNAS* 106:5622–26**

158. Reviews assays based on tube extrusion (both from giant vesicles and cells) to study dynamic processes occurring in cell membranes.

180. Provides important formalism for experiments on curvature sensing and generation.

181. Sorre B, Callan-Jones A, Manzi J, Goud B, Prost J, et al. 2012. Nature of curvature coupling of amphiphysin with membranes depends on its bound density. *PNAS* 109:173–78
182. Stachowiak JC, Hayden CC, Sasaki DY. 2010. Steric confinement of proteins on lipid membranes can drive curvature and tubulation. *PNAS* 107:7781
183. Stachowiak JC, Richmond DL, Li TH, Brochard-Wyart F, Fletcher DA. 2009. Inkjet formation of unilamellar lipid vesicles for cell-like encapsulation. *Lab Chip* 9:2003–9
184. Stachowiak JC, Richmond DL, Li TH, Liu AP, Parekh SH, Fletcher DA. 2008. Unilamellar vesicle formation and encapsulation by microfluidic jetting. *PNAS* 105:4697–702
185. Stachowiak JC, Schmid EM, Ryan CJ, Ann HS, Sasaki DY, et al. 2012. Membrane bending by protein–protein crowding. *Nat. Cell Biol.* 14:944–49
186. Stein H, Spindler S, Bonakdar N, Wang C, Sandoghdar V. 2017. Production of isolated giant unilamellar vesicles under high salt concentrations. *Front. Physiol.* 8:63
187. Steinkühler J, Agudo-Canalejo J, Lipowsky R, Dimova R. 2016. Modulating vesicle adhesion by electric fields. *Biophys. J.* 111:1454–64
188. Steinkühler J, De Tillieux P, Knorr RL, Lipowsky R, Dimova R. 2018. Charged giant unilamellar vesicles prepared by electroformation exhibit nanotubes and transbilayer lipid asymmetry. *Sci. Rep.* 8:11838
189. Steinkühler J, Różycki B, Alvey C, Lipowsky R, Weigl TR, et al. 2019. Membrane fluctuations and acidosis regulate cooperative binding of ‘marker of self’ CD47 with macrophage checkpoint receptor SIRP α . *J. Cell Sci.* 132:jcs216770
190. Taylor P, Xu C, Fletcher PDI, Paunov VN. 2003. A novel technique for preparation of monodisperse giant liposomes. *Chem. Commun.* 14:1732–33
191. Tian AW, Capraro BR, Esposito C, Baumgart T. 2009. Bending stiffness depends on curvature of ternary lipid mixture tubular membranes. *Biophys. J.* 97:1636–46
192. Tsai FC, Stuhmann B, Koenderink GH. 2011. Encapsulation of active cytoskeletal protein networks in cell-sized liposomes. *Langmuir* 27:10061–71
193. Tsumoto K, Matsuo H, Tomita M, Yoshimura T. 2009. Efficient formation of giant liposomes through the gentle hydration of phosphatidylcholine films doped with sugar. *Colloids Surf. B Biointerfaces* 68:98–105
194. van Swaay D, deMello A. 2013. Microfluidic methods for forming liposomes. *Lab Chip* 13:752–67
195. Veatch SL, Cicuta P, Sengupta P, Honerkamp-Smith A, Holowka D, Baird B. 2008. Critical fluctuations in plasma membrane vesicles. *ACS Chem. Biol.* 3:287–93
196. Veatch SL, Keller SL. 2003. Separation of liquid phases in giant vesicles of ternary mixtures of phospholipids and cholesterol. *Biophys. J.* 85:3074–83
197. Veatch SL, Keller SL. 2005. Miscibility phase diagrams of giant vesicles containing sphingomyelin. *Phys. Rev. Lett.* 94:148101
198. Veatch SL, Keller SL. 2005. Seeing spots: complex phase behavior in simple membranes. *Biochim. Biophys. Acta Mol. Cell Res.* 1746:172–85
199. Vequi-Suplicy CC, Riske KA, Knorr RL, Dimova R. 2010. Vesicles with charged domains. *Biochim. Biophys. Acta Biomembr.* 1798:1338–47
200. Vitkova V, Mitkova D, Antonova K, Popkirov G, Dimova R. 2018. Sucrose solutions alter the electric capacitance and dielectric permittivity of lipid bilayers. *Colloids Surf. A Physicochem. Eng. Aspects* 557:51–57
201. Vlahovska PM, Gracia RS, Aranda-Espinoza S, Dimova R. 2009. Electrohydrodynamic model of vesicle deformation in alternating electric fields. *Biophys. J.* 96:4789–803
202. Walde P, Cosentino K, Engel H, Stano P. 2010. Giant vesicles: preparations and applications. *ChemBioChem* 11:848–65
203. Waugh R, Hochmuth R. 1987. Mechanical equilibrium of thick, hollow, liquid membrane cylinders. *Biophys. J.* 52:391–400
204. Weinberger A, Tsai FC, Koenderink GH, Schmidt TF, Itri R, et al. 2013. Gel-assisted formation of giant unilamellar vesicles. *Biophys. J.* 105:154–64
205. Weiss M, Frohnmayer JP, Benk LT, Haller B, Janiesch J-W, et al. 2018. Sequential bottom-up assembly of mechanically stabilized synthetic cells by microfluidics. *Nat. Mater.* 17:89–96

198. Provides a review on phase diagrams of binary and ternary lipid mixtures.

206. Wick R, Walde P, Luisi PL. 1995. Light-microscopic investigations of the autocatalytic self-reproduction of giant vesicles. *J. Am. Chem. Soc.* 117:1435–36
207. Wollert T, Wunder C, Lippincott-Schwartz J, Hurley JH. 2009. Membrane scission by the ESCRT-III complex. *Nature* 458:172–77
208. Yamamoto T, Aranda-Espinoza S, Dimova R, Lipowsky R. 2010. Stability of spherical vesicles in electric fields. *Langmuir* 26:12390–407
209. Yu M, Lira RB, Riske KA, Dimova R, Lin H. 2015. Ellipsoidal relaxation of deformed vesicles. *Phys. Rev. Lett.* 115:128303
210. Zhao J, Wu J, Heberle FA, Mills TT, Klawitter P, et al. 2007. Phase studies of model biomembranes: complex behavior of DSPC/DOPC/cholesterol. *Biochim. Biophys. Acta* 1768:2764–76
211. Zhao J, Wu J, Veatch SL. 2013. Adhesion stabilizes robust lipid heterogeneity in supercritical membranes at physiological temperature. *Biophys. J.* 104:825–34
212. Zimmerberg J, Kozlov MM. 2005. How proteins produce cellular membrane curvature. *Nat. Rev. Mol. Cell Biol.* 7:9

Contents

Molecular Fitness Landscapes from High-Coverage Sequence Profiling <i>Celia Blanco, Evan Janzen, Abe Pressman, Ranajay Saba, and Irene A. Chen</i>	1
Split Green Fluorescent Proteins: Scope, Limitations, and Outlook <i>Matthew G. Romei and Steven G. Boxer</i>	19
How Good Can Single-Particle Cryo-EM Become? What Remains Before It Approaches Its Physical Limits? <i>Robert M. Glaeser</i>	45
Membrane Electroporation and Electropermeabilization: Mechanisms and Models <i>Tadej Kotnik, Lea Rems, Mounir Tarek, and Damijan Miklavčič</i>	63
Giant Vesicles and Their Use in Assays for Assessing Membrane Phase State, Curvature, Mechanics, and Electrical Properties <i>Rumiana Dimova</i>	93
Figure 1 Theory Meets Figure 2 Experiments in the Study of Gene Expression <i>Rob Phillips, Nathan M. Belliveau, Griffin Chure, Hernan G. Garcia, Manuel Razo-Mejia, and Clarissa Scholes</i>	121
Mammalian Respiratory Complex I Through the Lens of Cryo-EM <i>Abmed-Noor A. Agip, James N. Blaza, Justin G. Fedor, and Judy Hirst</i>	165
Single-Molecule Studies on the Protein Translocon <i>Anne-Bart Seinen and Arnold J.M. Driessen</i>	185
Mechanisms of Sensory Discrimination: Insights from <i>Drosophila</i> Olfaction <i>Lukas N. Groschner and Gero Miesenböck</i>	209
How the Genome Folds: The Biophysics of Four-Dimensional Chromatin Organization <i>Jyotsana J. Parmar, Maxime Woringer, and Christophe Zimmer</i>	231

Helicase Mechanisms During Homologous Recombination in <i>Saccharomyces cerevisiae</i> <i>J. Brooks Crickard and Eric C. Greene</i>	255
Generalized Born Implicit Solvent Models for Biomolecules <i>Alexey V. Onufriev and David A. Case</i>	275
An NMR View of Protein Dynamics in Health and Disease <i>Ashok Sekhar and Lewis E. Kay</i>	297
Biophysics of Chromatin Dynamics <i>Beat Fierz and Michael G. Poirier</i>	321
Raman Imaging of Small Biomolecules <i>Yibui Shen, Fanghao Hu, and Wei Min</i>	347
Polarizable Force Fields for Biomolecular Simulations: Recent Advances and Applications <i>Zhifeng Jing, Chengwen Liu, Sara Y. Cheng, Rui Qi, Brandon D. Walker, Jean-Philip Piquemal, and Pengyu Ren</i>	371
Programming Structured DNA Assemblies to Probe Biophysical Processes <i>Eike-Christian Wamhoff, James L. Banal, William P. Bricker, Tyson R. Shepherd, Molly F. Parsons, Rémi Veneziano, Matthew B. Stone, Hyungmin Jun, Xiao Wang, and Mark Bathe</i>	395
Understanding the Role of Lipids in Signaling Through Atomistic and Multiscale Simulations of Cell Membranes <i>Moutusi Manna, Tuomo Nieminen, and Ilpo Vattulainen</i>	421
Interrogating the Structural Dynamics and Energetics of Biomolecular Systems with Pressure Modulation <i>Roland Winter</i>	441
Regulation of Transmembrane Signaling by Phase Separation <i>Lindsay B. Case, Jonathon A. Ditlev, and Michael K. Rosen</i>	465
RNA-Mediated Virus Assembly: Mechanisms and Consequences for Viral Evolution and Therapy <i>Reidun Twarock and Peter G. Stockley</i>	495
Structure and Assembly of the Nuclear Pore Complex <i>Bernhard Hampoelz, Amparo Andres-Pons, Panagiotis Kastiris, and Martin Beck</i>	515
Hybrid Live Cell-Supported Membrane Interfaces for Signaling Studies <i>Kabir H. Biswas and Jay T. Groves</i>	537